Chain vol. 2, no. 2, pp. 1–XX, 2025
DOI:10.23919/CHAIN.2025.000006
ISSN 2097-3470
CN 10-1915/TB
Review Article

First-principles calculations innovation in wide bandgap semiconductors: Multiphysics field coupling and functional device design

Jie Wang[1], Yizhang Wu[2,3,✉], Hefang Cao[1], Yong Wang[4,✉], and Aimei Zhang[1,✉]

[1] *College of Mechanics and Engineering Science, Hohai University, Nangjing 211100, China*
[2] *Department of Applied Physical Sciences, The University of North Carolina at Chapel Hill, Chapel Hill, NC 27514, USA*
[3] *Institute of Materials Engineering, Nanjing University, Nantong 226019, China*
[4] *Wide Bandgap Semiconductor Technology Disciplines State Key Laboratory, School of Microelectronics, Academy of Advanced Interdisciplinary Research, Xidian University, Xi'an 710071, China*

Received: 11 March 2025
Revised: 20 March 2025
Accepted: 20 March 2025
Online: 3 April 2025

KEYWORDS
wide bandgap semiconductors, first-principles calculations, machine learning, defect engineering, multiscale modeling

ABSTRACT
Wide bandgap semiconductors have become the core material system for high-power electronic devices, deep-ultraviolet optoelectronic devices, and quantum information technology, featuring high-temperature stability and optoelectronic properties. First-principles calculations play an irreplaceable role in revealing the intrinsic physical properties of materials, guiding the optimization of energy-band engineering, and predicting the performance of devices through accurate modeling at the quantum mechanical level. This paper systematically reviews the key advances of first-principles calculations in wide bandgap semiconductor research in recent years: from the theoretical breakthroughs in electronic structure calculation and bandgap correction to the multiscale modeling of photoexcitation dynamics and thermal transport behavior; from the innovative design of defect formation mechanisms and doping strategies to the prediction of the performance of low-dimensional materials and heterojunction devices. The review shows that by integrating multi-body perturbation theory, machine learning algorithms, and dynamic simulation technology, first-principles calculations promote the paradigm shift from empirical exploration to theory-driven research on wide bandgap semiconductors, and the material-performance-device-function correlation model established by the study will lay the theoretical foundation for the breakthrough development of new-generation semiconductor technology.

Address correspondence to Yizhang Wu, yizhwu@unc.edu; Yong Wang, yongwang@xidian.edu.cn; Aimei Zhang, amzhang2009@hhu.edu.cn

有科出版 YOUKE PUBLISHING
EXCLUSIVELY AVAILABLE VIA IEEE Xplore DIGITAL LIBRARY

1 Introduction

Wide bandgap semiconductors (WBG) are semiconductor materials with a bandgap between 2 and 4 eV. Compared to conventional materials such as silicon (Si) and gallium arsenide (GaAs), WBGs show significant advantages in extreme environments such as high temperature, high frequency, high power, and radiation. WBGs have higher breakdown voltage, wider operating temperature range, higher radiation resistance, and higher current carrying capacity, and therefore have important applications in high-power electronics, optoelectronics, quantum computing, and other fields [1–9]. For instance, gallium nitride (GaN) is widely used in blue light-emitting diodes (LEDs) and high-frequency power devices due to its high electron mobility and wide bandgap (approximately 3.4 eV) [4, 10, 11]; silicon carbide (SiC) plays a key role in electric vehicles, renewable energy sources, and high-frequency power electronics due to its high thermal conductivity, high voltage resistance, and high-temperature stability [1, 12, 13]. The remarkable properties of these materials are gradually replacing traditional silicon materials in high-performance electronics. This is especially evident in high-power, extreme temperature, and high-frequency applications, which demonstrates unrivalled advantages.

The application of these materials can drive modern electronics toward higher efficiency, greater stability, and higher operating temperatures. However, research into wide bandgap semiconductors still faces challenges, particularly in the fields of material growth, defect control, device design, and commercial production. As the understanding of the nature of these materials continues to deepen, first-principles calculations are becoming an increasingly important tool for the study and design of wide bandgap semiconductors [14–19]. Using first-principles calculations, such as the density functional theory (DFT), researchers can delve deeper into the electronic structure, bandgap, optical properties, defect characteristics, and doping effects of these materials. These calculations provide a theoretical basis for the optimal design and performance prediction of materials, which can help to develop new semiconductor materials and improve the performance of existing materials.

First-principles calculations, particularly DFT, have been extensively utilized in the field of wide-bandgap semiconductors. Initially, DFT was predominantly employed for electronic structure calculations of materials, thereby facilitating scientists' comprehension of the fundamental electronic properties of these materials. However, with the improvement of computational power and the advancement of computational methods, DFT has been gradually extended to the fields of bandgap prediction, doping optimization, and defect engineering for wide bandgap semiconductors. In recent years, the GW approximation method has effectively improved the error of DFT in bandgap prediction, making the electronic structure calculation of wide bandgap semiconductors more accurate [20–22]. Through DFT calculations, researchers can predict the band gap, conduction band, and valence band structures of materials and investigate the effects of doping and defects on their properties [23, 24]. This enables the optimization of electronic and optoelectronic characteristics. The combination of DFT and GW methods is also crucial for studying a material's optical and thermal properties. Under extreme conditions, such as high temperatures and frequencies, first-principles calculations can reveal changes in material stability and properties, providing a theoretical foundation that supports the improvement of device design [25, 26]. In the field of wide bandgap semiconductors, first-principles calculations go beyond theoretical exploration, acting as a crucial tool in developing practical materials and device design. Researchers can optimize existing materials or design entirely new wide bandgap semiconductors by carefully analyzing materials' electronic structure, optical properties, and thermal behavior [27]. This approach significantly improves the performance of wide bandgap semiconductors in high-power electronics, optoelectronics, radio frequency devices, and other applications, driving the advancement of semiconductor technology [28]. With the continued growth of computational power and the development of new algorithms, first-principles calculations will remain instrumental in advancing both the research and practical applications of wide bandgap semiconductors.

Rapid advancements in wide bandgap semiconductors have ushered in a new era of research centered on the design of innovative materials, the development

of high-performance devices, and the optimization of computational techniques. As computational models and methods continue to evolve, first-principles calculations have become an indispensable tool for studying wide bandgap semiconductor materials. This progress has, in turn, driven sustained advancements in electronics, optoelectronics, and other cutting-edge technologies.

This review systematically sorts out the key advances of first-principles calculations in wide bandgap semiconductor research and its multiscale application framework. By integrating density functional theory, multibody perturbation theory, and machine learning methods, we focus on constructing a complete chain of theoretical systems from analyzing fundamental physical properties to the functional design of devices. The research systematically elaborates the methodological breakthroughs in the core directions, such as accurate calculation of electronic structure, modeling of optical-electrical coupling mechanism, prediction of thermal transport properties, and development of defect regulation strategies, revealing the role of quantum mechanical computational methods in bridging the correlation between intrinsic properties and macroscopic performance of materials. In particular, novel solutions based on multiscale computation are proposed for key scientific problems such as energy band engineering, interfacial effects, and carrier dynamics in third-generation semiconductor materials. In addition, the innovative impact of computational materials science on wide bandgap semiconductor research is discussed: at the level of fundamental theory, the synergistic characterization of the exciton effect and carrier transport is realized through the development of the coupled algorithm of the non-equilibrium Green's function and the Bethe-Salpert equation; at the level of material design, the synergistic screening model of high-throughput computational machine learning has been developed, which has significantly improved the discovery efficiency of new low-dimensional semiconductor materials. At the level of device optimization, we have developed atomically accurate interface modeling techniques that provide microscopic mechanism analysis for heterojunction energy band modulation. These theoretical advances not only deepen the understanding of the physical nature of broadband semiconductors but also lay a solid computational foundation for materials innovation for high-power electronic devices, deep-ultraviolet optoelectronic systems, and quantum information technology and promote semiconductor research to enter a new stage of "predictable design".

2 Application of first-principles calculations to wide bandgap semiconductors

2.1 Electronic structure calculation

Electronic structure calculations are essential for understanding and optimizing the properties of semiconductor materials, particularly in the study of wide bandgap semiconductors, where accurate bandgap prediction is crucial. First-principles calculations enable researchers to analyze the electronic structure of these materials in detail, including the energy band structure, the density of electronic states (DOS), and the position of the Fermi energy levels. The results of these calculations offer a theoretical foundation for optimizing material properties, which is especially important for precise bandgap prediction and modulation.

In recent years, significant progress has been made in the electronic structure calculations of wide bandgap semiconductors, driven largely by continuous advancements in computational methods and resources. The use of DFT and the GW approximation in bandgap calculations has notably advanced the study of these materials. As the most widely used first-principles method, DFT accurately describes the ground state's electronic structure. However, due to its approximations in handling electron exchange-correlation effects, DFT often underestimates the bandgap of wide bandgap semiconductors, particularly for materials such as GaN, SiC, and ZnO [29–32]. In these cases, the DFT-calculated bandgap tends to be lower than the experimental value. To address this, researchers commonly apply the GW approximation to correct the bandgap and improve the accuracy of predictions.

As shown in Figs. 1(a) and 1(b), the band gap of 3C-SiC was calculated by Perdew-Burke-Ernzerhof (PBE) functional, and the result obtained was 1.4 eV. Still, after considering the GW approximation, the

band gap calculated by the G_0W_0 method was 2.3 eV, which is very close to the experimental value of 2.36 eV [29]. In the discussion of the band gap of $(ZnO)_{1-x}(GaN)_x$ alloy by Olsen et al., a GW approximation was used to calculate the band gap of the system, and the results are shown in Fig. 1(c), which are in good agreement with the experimental values [32]. The GW approximation is a many-body perturbation theory based on the one-body Green's function, which provides a more rigorous framework for describing electronic structure than conventional methods [33–37]. At its core is the exchange-correlation self-energy function, which is analogous to the exchange-correlation potential in the Kohn-Sham density functional theory. Unlike the exchange-correlation potential, the exchange-correlation self-energy is a spatially nonlocal, energy-dependent, non-Emilian function that includes all non-classical electronic interaction effects beyond the Hartree approximation. The photoelectron spectrum (PES) and inverse photoelectron spectrum (IPS) associated with the quasiparticle excitation energy spectrum can be obtained directly from the self-energy function, and these energy spectra can be measured experimentally. The exact self-energy function follows a set of self-consistently coupled integral differential equations known as the Hedin equation [36, 38]. However, since the solution of this equation is extremely difficult to find in complex systems, approximations must be introduced in practical applications. The most commonly used approximation is the GW approximation, in which the self-energy function in the time-space domain is expressed as the product of the one-body Green's function G and the shielding Coulomb action W. The GW approximation is used to solve the Hedin equation. Although the GW approximation provides an effective computational framework, the numerical solution of the Hedin equation still faces the challenges of complex program implementation and high computational complexity. In practical studies, a commonly used approximation is the G_0W_0 method, in which G and W are calculated based on the single-electron orbital energy and wave function, respectively, at some mean-field approximation (H_0) [39].

The GW approximation method enhances the DFT, thereby improving the accuracy with which it characterizes the dynamic effects of electrons and significantly improving the accuracy of bandgap prediction [41, 42]. Recent studies have demonstrated that the GW method has become a standard and effective tool for bandgap prediction in wide bandgap materials. Rinke et al. applied the GW approximation to correct the bandgap of GaN, finding that it more accurately matched experimental results compared to DFT, which underestimated the bandgap [41]. Notably, temperature effects also play a critical role in bandgap modulation. As demonstrated by Lee et al., the electronic structure of β-Ga_2O_3 exhibits significant temperature dependence due to electron-phonon interactions and thermal

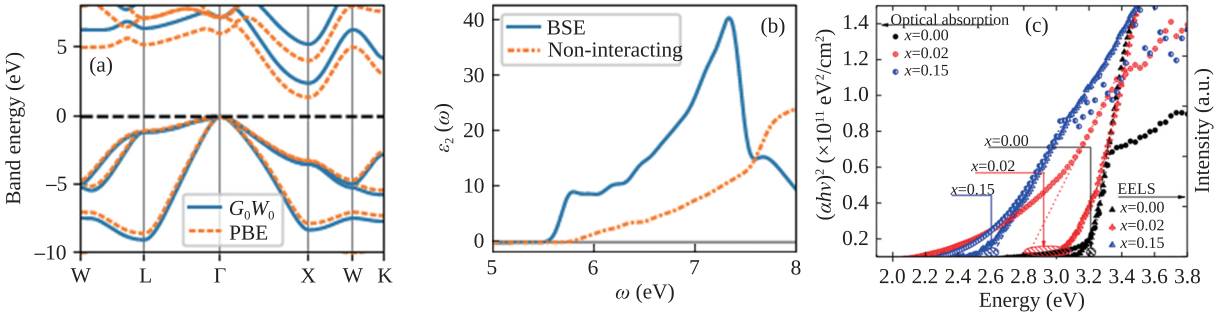

Figure 1 (a) Quasiparticle band structure of pristine 3C-SiC computed within DFT using Perdew-Burke-Ernzerhof (PBE) functional and within the GW approximation. (b) Comparison between the imaginary part of the dielectric function calculated with GW-Bethe-Salpeter equation (GW-BSE) and with the noninteracting particle approximation. A Gaussian smearing of 0.05 eV is used for calculating the dielectric function. Reproduced with permission from Ref. [29]. © 2022, the American Physical Society. (c) Optical absorption and electron energy loss spectra for x=0, 0.02, and 0.15, see corresponding symbols in the legend. The optical data are presented in the form of Tauc plots assuming direct allowed transitions, while the EELS data are linearly scaled. Dotted (optical absorption) and dashed (EELS) lines represent an extrapolation of the linear region intersecting the x-axis. The point of intersection marks E_g. Reproduced with permission from Ref. [40]. © 2019, The American Physical Society.

expansion [42]. Their combined first-principles and experimental study revealed a bandgap reduction of over 0.5 eV between 0 and 900 K (Fig. 2), with electron-phonon renormalization identified as the dominant mechanism. This work highlights the necessity of incorporating temperature effects alongside advanced exchange-correlation corrections for accurate bandgap predictions in device-operating conditions. The study achieved a more accurate energy band structure by combining the GW method with DFT, providing a theoretical basis for optimizing GaN's performance in high-power applications.

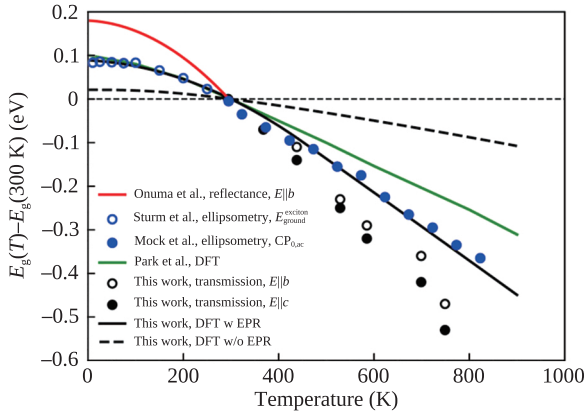

Figure 2 Change in the bandgap of β-Ga_2O_3 as a function of temperature from T=0 to 900 K. For ease of comparison to other experimental and computational results, changes in the gap are referenced to the T=300 K value. Reproduced with permission from Ref. [42]. © 2023, AIP Publishing.

In addition to the traditional DFT and GW methods, hybrid functional approaches have been widely adopted in recent years for studying wide bandgap semiconductors. By incorporating nonlocal exchange-correlation functions, these methods effectively enhance the accuracy of bandgap calculations, addressing the limitations of DFT [43].

Back in the 1990s, Becke, together with Bylander and Kleinman, almost simultaneously proposed the introduction of a nonlocal exchange-correlation potential to make corrections to the electronic structure of the system [43, 44]. This approach is no longer limited to the Kohn-Sham theoretical framework. Seidl et al. later systematized this approach [45]. They changed the definition of the single reference. This redefinition ensured the approach was strictly unified within the DFT framework. It led to the development of generalized Kohn-Sham (GKS) theory. These methods perform well in specific cases. However, they still fail significantly in calculations of total energy and other properties.

In recent years, high-throughput computing and machine learning methods have gradually become popular directions in wide bandgap semiconductor research. And artificial intelligence based on big language models is also shining in the industrial sector [46]. By combining high-throughput computing and machine learning, researchers can more efficiently screen materials with excellent properties [47–54]. A methodology paradigm that has demonstrated cross-domain effectiveness in fields ranging from wearable sensor optimization to robotic motion control systems [55, 56]. For example, Chen et al. utilized pymatgen and matminer to extract data from the Materials Project, encompassing 3720 ABX_3-type compounds and 2660 $A_2B(I)B(II)X_6$-type compounds. This effort enabled the identification of key material characteristics with accurately predicted band gaps and formation energies. To estimate missing data, the random forest algorithm was employed, followed by using tolerance and octahedral factors to screen for stable chalcogenide structures, thereby improving data quality. A subsequent SHAP (SHapley Additive exPlanation) analysis was performed to determine the most influential descriptors. The results indicate that higher formation energies, a large number of transition metals, and a considerable presence of d-orbital valence electrons are critical for forming narrow bandgap perovskites. In contrast, a higher number of *f*-orbital electrons and large electronegativity differences between elements contribute to the formation of wide bandgap perovskites. Additionally, Shen et al. developed a hierarchical material screening framework (HMSF) to identify ultra-wide bandgap materials. The framework is similar to graph-based path-planning strategies in robotic systems [57]. They established a correlation between material chemistry and properties and adjusted hyperparameters in the machine-learning algorithm to enhance prediction accuracy via Bayesian optimization. This approach led to the discovery of four previously unknown ultra-wide bandgap materials characterized by suitable forbidden bandwidths,

exceptional thermal stability, a pronounced deep ultraviolet optical response, and low electronic effective masses. These achievement highlights the significant potential of machine learning in accelerating material design.

In the study of semiconductor materials, it has been found that introducing defects and doping, among other things, has a significant effect on the electronic structure of semiconductors. For example, co-doping and Co-Al Co-doping in ZnO were discussed by Khan et al. It was found that after Co doping, the material exhibited antiferromagnetism, while after Co Al co-doping, there was a transformation of the antiferromagnetic phase into a ferromagnetic phase, and the energy of the antiferromagnetic state was higher than that of the ferromagnetic phase by 184 meV, which is much higher than the thermal motion energy at room temperature [58]. With this energy difference, the Curie temperature of the system was calculated by mean-field theory to be 690 K. Meanwhile, the optical absorption spectrum shows, with the increase of Co concentration, the band gap of ZnO and the position of the d-d transition peak of Co ions show blueshifts and redshifts behaviors, respectively; with the Co concentration increases, the intensity and width of the d-d transition peaks decrease. In addition, Co Al co-doping not only increases the band gap but also generates new absorption peaks in the infrared and visible regions. This work demonstrates the modulation of ZnO optoelectronic and magnetic properties by Co doping and Co Al co-doping. It provides theoretical support for applying ZnO-based materials in future electronic and optoelectronic devices. Beyond chemical modifications, environmental factors such as temperature also profoundly reshape electronic properties. Lee et al. demonstrated that thermal lattice vibrations in β-Ga_2O_3 induce band edge localization, particularly for the valence band maximum (VBM), as shown in their charge density isosurfaces (Fig. 3) [42]. This localization leads to increased hole effective masses at elevated temperatures, directly impacting carrier mobility and device performance. Such findings emphasize the interplay between intrinsic defects, extrinsic dopants, and thermodynamic conditions in determining semiconductor behavior.

First-principles calculations have played a crucial role in the study of the electronic structure of wide bandgap semiconductors, and significant progress has been made in the prediction and optimization of the bandgap. By using advanced computational methods such as DFT, GW approximation, and hybrid functional methods, researchers can gain a deeper understanding of the electronic properties of wide

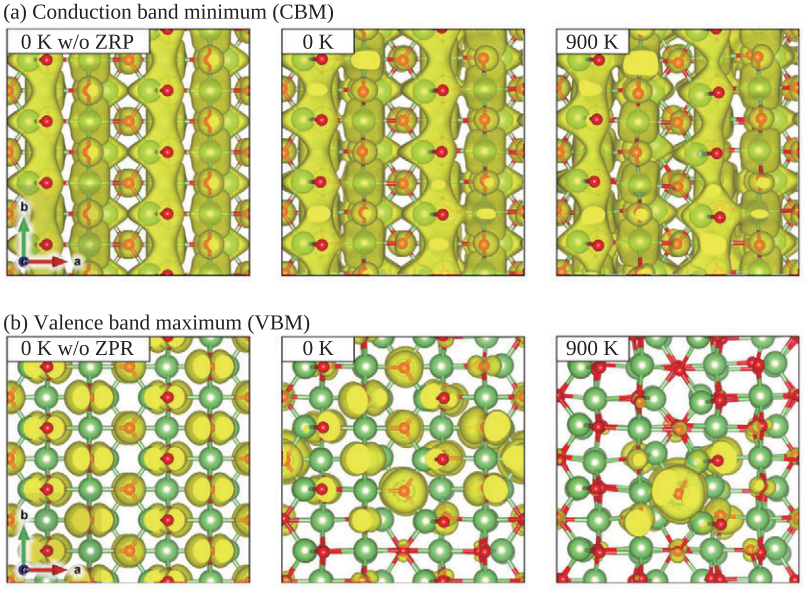

Figure 3 Three-dimensional isosurfaces of charge densities of the (a) CBM and (b) VBM from one-shot configurations of β-Ga_2O_3 at T= 0 K without ZPR, 0 K with zero-point renormalization (ZPR), and 900 K. All isosurfaces are shown at the value of 1.5 × 10^{-4} e/Å^3. Reproduced with permission from Ref. [42]. © 2023, AIP Publishing.

bandgap semiconductors. In addition, emerging research methods such as high-throughput computing, machine learning, and defect engineering offer more opportunities for material design and performance optimization. With continued improvements in computational accuracy and the emergence of new methods, researchers are able to more precisely control the electronic properties of wide bandgap semiconductors, providing a solid theoretical foundation for their applications in fields such as high-power electronics, optoelectronics, and quantum computing.

2.2 Calculation of optical properties

Optical properties are one of the important characteristics of wide bandgap semiconductors, as they directly determine the potential applications of these materials in optoelectronic devices, including photodetectors, lasers, solar cells, and light-emitting diodes [59–61]. Through first-principles calculations, researchers can analyze the optical response of materials in detail, including absorption spectra, reflectance, and optical bandgap. This, in turn, provides theoretical support for the optimization of the materials' optoelectronic properties. The optical properties of wide bandgap semiconductors are closely related to their electronic structures; therefore, accurate prediction of optical properties is crucial for the design and application of the materials [62–64].

The accurate calculation of the optical properties of materials by DFT, especially the calculation and prediction of absorption spectra and optical bandgap, has gradually become a research hotspot. The GW-BSE method has an important position in this field and has become one of the standard methods for predicting optical properties. The GW-BSE method is a computational approach grounded in many-body perturbation theory, which is employed to investigate the quasiparticle and optical characteristics of materials [65–67]. It combines the GW approximation and the Bethe-Salpeter equation (BSE) to accurately calculate the bandgap and exciton properties of materials from first principles. The GW approximation, as previously mentioned, is a method used to calculate the quasiparticle properties of materials by approximating the electron self-energy to the quasiparticle energy and wave function. It is able to provide more accurate band gap values than conventional DFT. The BSE is mainly used to study the optical properties of materials, especially exciton effects. It has been demonstrated to be a highly effective tool for predicting the optical response of materials by considering the electron-hole interaction [68–70]. The BSE approach treats the electron-hole pair as a whole, known as an exciton, and calculates the energy and wave function of its excited state. The GW-BSE method integrates the GW approximation and BSE, enabling the simultaneous consideration of quasiparticle and exciton effects. It is widely regarded as one of the most precise methodologies for calculating quasiparticle and optical properties of condensed matter systems [65, 67, 71, 72]. Holzer et al. investigated how GW-BSE can be used to calculate molecular excitation energies in strong magnetic fields. They extend the application of these methods by introducing the Bethe-Salpeter equation with the GW approximation into calculations in strong magnetic fields. They also provide a new computational framework that can accurately describe molecular excitation energies and optical properties in the presence of strong magnetic fields [71]. In addition, the work is compared with reference data on the excited energies of the triplet states of 36 small to medium-sized molecules. The results verify the validity of the method under strong magnetic fields, demonstrating the significant effect of strong magnetic fields on the optical properties of molecules. Excitation energy calculations for different molecules under strong magnetic field conditions yielded significant changes in the optical properties. As demonstrated in Fig. 4, the color of tetracene undergoes a transition from orange to green as the magnetic field strength increases from 0 to 9000 T. This color change can be accurately predicted by the GW-BSE method. The calculation of the excitation energy of a strong magnetic field based on the GW-BSE method proposed by Holzer et al. establishes a novel theoretical framework for the study of the optical properties of molecules in extreme environments. This work not only expands the application of the GW-BSE method but also provides a powerful tool for the accurate characterization of the optical properties of molecules under strong magnetic fields. Future studies can build on this foundation to further explore the excitation

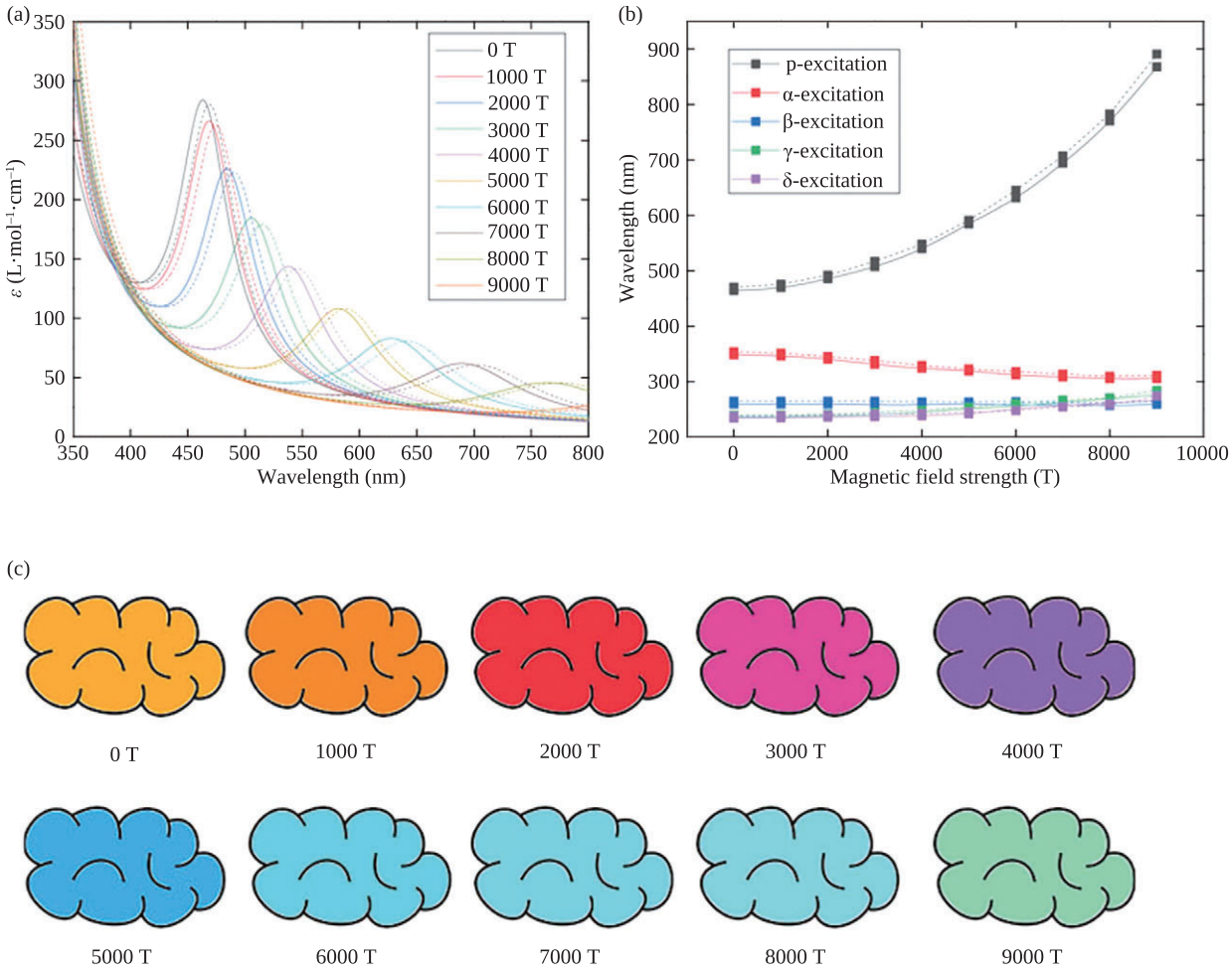

Figure 4 Magnetic Field Modulation of Tetracene's Optical Properties: Spectral Shifts, Excitation Wavelengths, and Color Evolution. (a) UV/vis spectra of tetracene as predicted at different magnetic field strengths between 0 T and 9000 T. Solid lines denote calculations using the CD-evGW(10)/BSE@BHLYP method while dashed lines denote CD-evGW(10)/BSE@CAM-B3LYP calculations. (b) Wavelengths of the relevant lowest vertical excitations of tetracene at different magnetic field strengths between 0 T and 9000 T. The p-excitation, which is predominantly responsible for the color of tetracene, is most affected by the external field. Solid lines denote calculations using the CD-evGW(10)/BSE@BHLYP method, while dashed lines denote CD-evGW(10)/BSE@CAM B3LYP calculations. (c) Color of tetracene as predicted at the CD-evGW(10)/BSE@CAM-B3LYP level of theory at different magnetic field strengths between 0 T and 9000 T. To obtain the depicted colors, the vertical excitations of the optical spectrum were broadened by 0.15 eV and converted into an RGB color code while the intensity was scaled relative to the zero-field by integrating over the visible region of the spectrum. Reproduced with permission from Ref. [71]. © 2021, Frontiers.

energy spectra and optical behaviors of different types of molecules, especially complex molecular systems, in high-intensity magnetic fields. With the continuous development of computational methods, combined with more efficient many-body theories and modern computational techniques, it is expected to be able to deal with larger and more complex molecular systems and to reveal the far-reaching effects of magnetic fields on the excitation energies of molecules.

The GW-BSE method has been successful in calculating the optical properties of materials. However, we should also pay attention to the selective modulation of optical properties by heterojunctions and strains, and so on [73–77]. Feng et al. found that the strain of the material can have an important effect on the optical properties. For example, Feng et al. studied the electronic and optical properties of van der Waals heterostructures stacked with g-ZnO and Janus-WSSe monolayers using VASP to calculate their properties [78]. They used the hybridized, generalized

HSE method to obtain more accurate band gap values. The electronic structure and band alignment of AB-stacked g-ZnO/Janus-WSSe heterostructures are discussed in the work. It is found that the configuration has a typical type II band alignment, i.e., the conduction band minimum (CBM) and the valence band maximum (VBM) are in different materials. This band alignment facilitates the separation of photogenerated electrons and holes, thus improving the photocatalytic efficiency. In addition, due to the difference in the figure of merit between g-ZnO and Janus-WSSe ($\Delta\Phi$ = 0.533 eV), electrons are transferred from the g-ZnO layer to the Janus-WSSe layer, forming an intrinsic built-in electric field. This built-in electric field promotes the separation of photogenerated electron-hole pairs, which enhances the photocatalytic efficiency. A similar enhancement mechanism was observed in the S-type heterojunction of amorphous/crystalline carbon nitride, where the optimized interfacial charge transfer led to a significant improvement in the reduction efficiency of CO_2 [79]. Interestingly, the optical absorption coefficients of the AA-stacked and AB-stacked heterostructures show unique characteristics under different strains. Negative stretching increases the ultraviolet (UV) absorption and decreases the visible absorption, while positive stretching decreases the UV absorption and increases the visible absorption. Furthermore, the AB-stacked g-ZnO/Janus-WSSe heterostructure exhibits excellent photocatalytic water decomposition. The photoexcited electrons were transferred to the conduction band of the Janus-WSSe layer, while the photoexcited holes were transferred to the valence band of the g-ZnO layer. In the Janus WSSe layer, the collected photoexcited holes can drive the generation of oxygen; in the g-ZnO layer, the collected photoexcited electrons can drive the generation of hydrogen.

van der Waals heterostructures can be formed by stacking different two-dimensional materials. The combination of two or more materials into a heterojunction can effectively modulate the electronic and optical properties of the material [80–83]. While heterostructure engineering focuses on interfacial effects, chemical doping provides an alternative pathway for optical tuning. He et al. systematically compared Cr doping positions (center, radius ½, surface) in ZnSe nanowires (NWs) (Fig. 5), revealing that mid-gap defect states from Cr(d)-Se(p) hybridization dominate absorption characteristics [84]. Their Bader charge analysis (Fig. 6) further shows localized charge redistribution around dopants, creating defect-induced absorption peaks distinct from heterojunction-mediated modifications. This approach often achieves a better result and is a hot research topic in the academic community. In 2023, Mustafa et al. investigated the electronic and optical properties of photodetectors based on multilayer graphene/MoS_2 heterostructures [85]. Their work systematically investigated the electronic and optical properties of multilayer graphene/MoS_2 heterostructures. The results show that the band gap of MoS_2 can be significantly tuned by introducing graphene layers, which can be reduced by up to 36.3 meV, making the heterostructures promising for applications in photodetectors. Meanwhile, the optical absorption coefficients of the graphene/MoS_2-based heterostructures are significantly enhanced in the visible to ultraviolet region, especially at 1551 nm (0.8 eV) and 1240 nm (1 eV), indicating an enhanced light absorption capability in these wavelength ranges. In addition, these heterostructures exhibit nonlinear optical behavior from the infrared to the visible region, which has important implications for photonic devices, especially photodetectors.

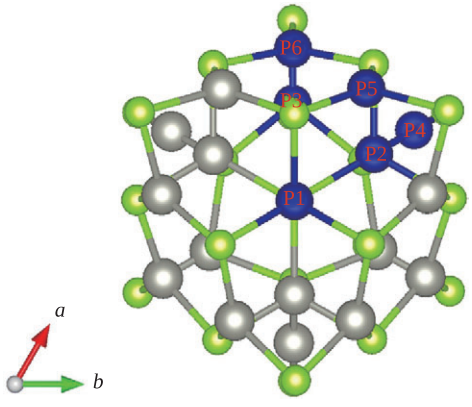

Figure 5 The cross-section of the optimized NW structure and all types of doping positions. The bule ball is Cr atoms. Reproduced with permission from Ref. [84]. © 2023, Elsevier.

From the above, we can realize that optical property calculations are the key to understanding and optimizing the optoelectronic performance of wide

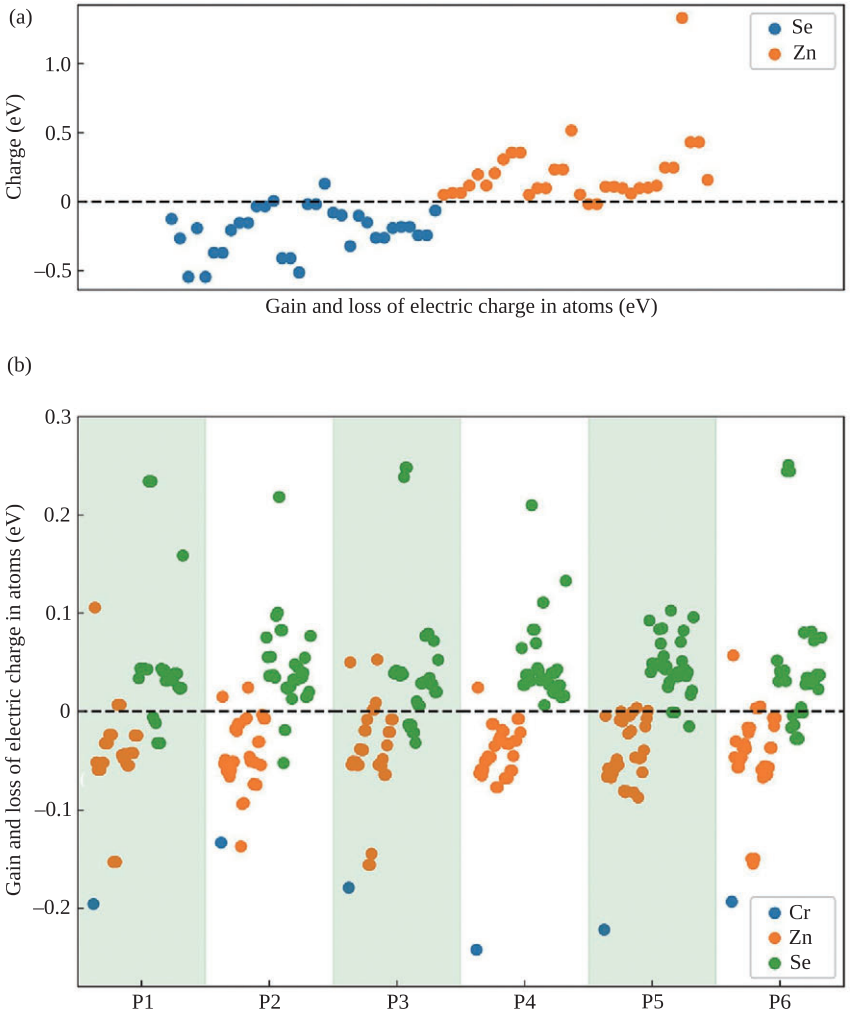

Figure 6 Bader charge analysis: (a) ZnSe NWs and (b) Cr^{2+}: ZnSe NWs. Reproduced with permission from Ref. [84]. © 2023, Elsevier.

bandgap semiconductors. With the advancement of computational methods, especially the application of GW-BSE method, researchers are able to predict the optical response of wide bandgap semiconductors more accurately. In addition, the influence of factors such as heterojunction, stress modulation, and surface interfacial effects on the optical properties has become a hot topic of current research. Through these studies, more accurate theoretical support and design guidance can be provided for the application of wide-bandgap semiconductors in optoelectronic devices.

2.3 Calculation of thermal properties

As one of the core research areas in condensed matter physics and materials science, the thermal properties of materials are directly related to key engineering and technological issues such as energy conversion efficiency, reliability of electronic devices, and thermal protection systems in aerospace. Traditional experimental methods for measuring thermal conductivity, thermal expansion coefficient, and lattice vibrational properties face many challenges: the difficulty of *in-situ* characterization under extreme conditions (high temperature/high pressure), the bottleneck of accurate quantification of the interfacial thermal resistance of low-dimensional materials, and the limitations in analyzing the heat transport mechanism of new complex compounds. In this context, first-principle computational methods, with their unique advantages based on the fundamental principles of quantum mechanics, have gradually emerged as an important research paradigm for revealing the microscopic mechanisms of the thermal properties of materials. It is well known that thermal properties are key indicators of the stability and application performance of wide bandgap

semiconductors in high-temperature environments [86–88]. Recent experimental breakthroughs in the thermal management of AlN further validate this thesis. Alvarez-Escalante et al. demonstrated that homoepitaxial AlN thin films achieve exceptional thermal conductivity up to 195.71 $W \cdot m^{-1} \cdot K^{-1}$ at 1 μm thickness (Fig. 7(a)), approaching 57% of the bulk theoretical value (340 $W \cdot m^{-1} \cdot K^{-1}$) [89]. Remarkably, their FDTR measurements revealed ultrahigh thermal boundary conductance (G) exceeding 2590 $MW \cdot m^{-2} \cdot K^{-1}$) for 3 μm films (Fig. 7(b)), attributed to atomic-level interface control via Al-assisted surface cleaning. This represents a 10-fold improvement over heteroepitaxial systems like GaN/SiC ($G \approx 230$ $MW \cdot m^{-2} \cdot K^{-1}$), effectively overcoming the interfacial resistance bottleneck in traditional low-dimensional materials. With the increasing application of semiconductor materials in high-power electronic devices, optoelectronic devices, and thermoelectric devices, it becomes particularly important to accurately calculate and optimize the thermal properties of materials, such as thermal conductivity, specific heat capacity, and thermal expansion [90–93]. Thermal properties are directly related to the thermal stability, thermal diffusivity, and energy conversion efficiency of materials at high temperatures [94, 95]. Therefore, first-principles calculations provide a powerful theoretical tool to study these properties and are especially indispensable in the design and performance optimization of wide bandgap semiconductor materials.

In 1996, Mahan and Sofo presented a study on maximizing the eutectic value of thermoelectric materials by optimizing the electronic structure [96]. They unified the electrical conductivity, thermal potential, and thermal conductivity as integrals of a transport distribution function and derived a mathematical function of the transport distribution that maximizes the optimum value. Specifically, they used the Boltzmann equation to describe the transport coefficients and introduced a transport distribution function related to the velocity, lifetime, and dispersion relations of the electron population. By using a transport distribution in the form of a delta function, the thermoelectric optimum can be maximized. This suggests that the electron energy distribution involved in the transport process should be as narrow as possible to achieve higher thermoelectric efficiency. This study provides a new theoretical perspective for the design of high-efficiency thermoelectric materials, which is of great significance for the subsequent improvement of the optimum value of thermoelectric materials.

In addition, DFT calculations show significant potential in the study of the thermal properties of 2D materials. Xu et al. found that nanohoneycomb-pleated PbTe monolayers have very low lattice thermal conductivity (0.75–0.79 $W \cdot m^{-1} \cdot K^{-1}$ at 900 K) and high electron

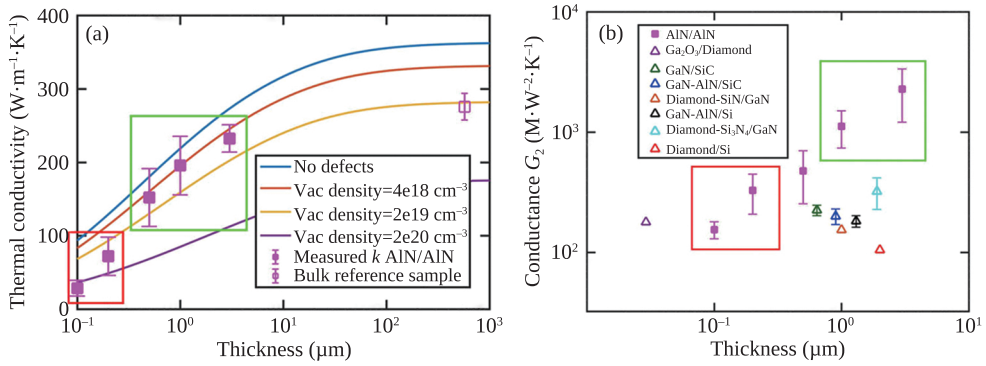

Figure 7 (a) Comparison between the calculated *k* based on first-principles calculations and measured *k* based on domain thermoreflectance (FDTR) (thickness dependence of AlN). The red square indicates homoepitaxially grown AlN samples impacted by surface pits (i.e., material defects), while the green square indicates homoepitaxially grown AlN samples with a negligible surface pit impact. (b) Comparison of thermal conductance among various WBG and ultra-wide bandgap (UWBG) thin films/substrate reports β-Ga_2O_3/diamond, GaN/SiC, GaN-AlN/SiC, GaN-AlN/Si, diamond-SiN/GaN, diamond-Si_3N_4/GaN, diamond/Si, and AlN/AlN (magenta squares, data by FDTR) from this work with respective error bars. The red square indicates homoepitaxially grown AlN samples impacted by surface pits (i.e., material defects). The green square indicates the ultrahigh G_2 of the 1 and 3 μm samples. Reproduced with permission from Ref. [89]. © 2022, AIP Publishing.

mobility (499.552 $cm^2 \cdot V^{-1} \cdot s^{-1}$) through an in-depth study of PbTe [97]. They calculated the phonon dispersion relation using density functional perturbation theory (DFPT), confirmed the kinetic stability of the system, and quantified the phonon scattering effect. The folded structure induces strong phonon anharmonicity, which reduces the lattice thermal conductivity at 900 K to 0.75–0.79 $W \cdot m^{-1} \cdot K^{-1}$, which is two orders of magnitude lower than that of conventional bulk materials. Combined with Boltzmann transport theory calculations, the system exhibits a Seebeck coefficient of 1.574 $mV \cdot K^{-1}$ and a thermoelectric figure of merit (ZT) of 1.55 in the 300–900 K range. The performance enhancement is mainly attributed to the optimization of carrier transport under electron-phonon coupling. This study has successfully established a theoretical correlation model from the atomic-scale electronic structure to the mesoscale thermal transport properties, which provides a quantitative research framework for the rational design of low-dimensional thermoelectric materials. Further, recent advances in structural design further demonstrate the versatility of 2D materials in thermal-electronic coupling. Zhao et al. systematically investigated strain-modulated anomalous thermal transport in porous buckled X-AlN (X=C, Si, TC) monolayers through evolutionary structural search and first-principles calculations [98]. As shown in Fig. 8(a) of their work, the lattice thermal conductivity of TC-AlN reached 123.75 $W \cdot m^{-1} \cdot K^{-1}$ at 300 K, 17 times higher than pristine AlN, due to strong covalent bonds suppressing out-of-plane phonon scattering. Remarkably, their Fig. 8(b) revealed a non-monotonic thermal conductivity response under biaxial strain: an initial increase peaking at 4% strain (165 $W \cdot m^{-1} \cdot K^{-1}$) followed by decline, arising from competition between enhanced N-N bond strength reducing anharmonicity and phonon mode softening at higher strains. This strain-engineered thermal switching mechanism provides new insights for dynamically controlling heat dissipation in semiconductor devices. Notably, reducing the dimensionality of the material to two dimensions has also been shown to be an effective way to improve the thermodynamic stability. Li et al. predicted two BeH_2 monolayer structures (α-BeH_2 and β-BeH_2) by performing a global search via a particle swarm optimization method and found that these two structures have high thermodynamic stability and mechanical strength [99]. The study also unexpectedly found that α-BeH_2 has a negative Poisson's ratio, which is rare in 2D materials. Since the beryllium hydride monolayer has the same number of electrons as graphene, its 2D structure is highly feasible in experiments, which provides a strong theoretical basis for the experimental preparation of monolayer BeH_2. The above studies have successfully revealed the microscopic mechanism of the material properties at the theoretical level, providing a new perspective for further understanding the physical connotation of the materials.

The thermal properties of materials are a key area of research in condensed matter physics and materials

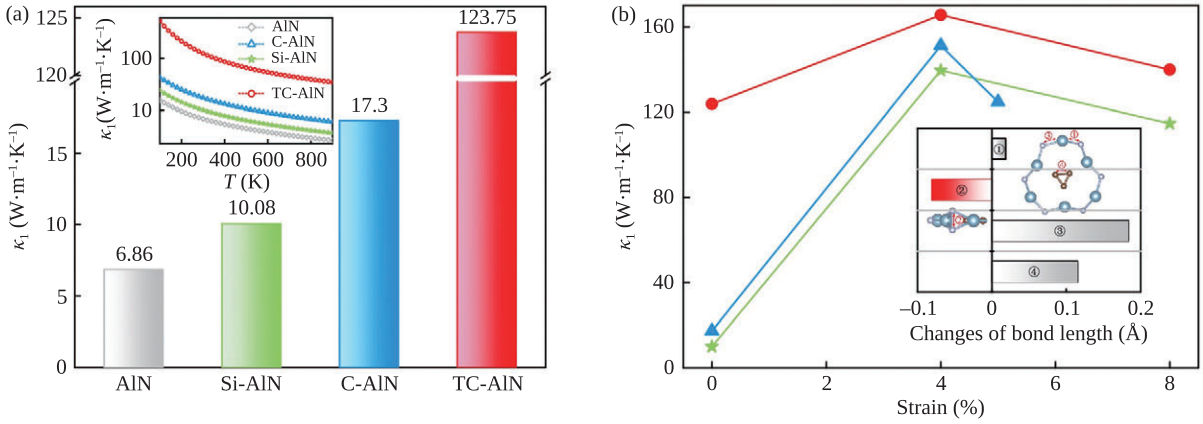

Figure 8 Strain modulates lattice thermal conductivity in holey crumpled AlN systems and reveals doping-dependent responses under varying strains. (a) Lattice thermal conductivity at 300 K of holey crumpled surface, AlN vs. X-AlN (X=C, Si, TC). (b) Lattice thermal conductivity of X-AlN (X=C, Si, TC) at 300 K at different strains. Reproduced with permission from Ref. [98]. © 2023, Science Press.

science, directly affecting the efficiency of energy conversion and a wide range of engineering applications. In polymer nanocomposites, morphologically tailored nanostructures have been shown to achieve exceptional breakdown field strength (>10 MV·cm^{-1}) alongside giant electrocaloric effects, illustrating the universal value of microstructure design in thermal-electrical property optimization [100]. Traditional experimental methods have significant limitations in *in-situ* characterization under extreme conditions of high temperature and pressure, in quantifying thermal resistance at low-dimensional material interfaces, and in resolving heat transport mechanisms in complex materials. First-principles calculation, with its essential advantages based on quantum mechanics, provides a powerful tool for revealing the microscopic mechanisms of the thermal properties of materials. It is particularly important for the systematic understanding of thermal properties such as thermal conductivity, specific heat capacity, and thermal expansion of materials. Through first-principles calculations, the thermal behavior of materials in complex environments can be accurately predicted, and on this basis, materials design and performance optimization can be carried out, providing theoretical basis and guidance for the research and development of high-efficiency thermoelectric materials, wide-bandgap semiconductors, and novel low-dimensional materials, and promoting the continuous development of the frontiers of materials science.

2.4 Doping and defect engineering

Doping and defect engineering is a fundamental strategy for optimizing the performance of wide bandgap semiconductors. This approach is achieved through precise control of energy band structures, effective modulation of carrier concentrations, and strategic management of surface states, etc., which collectively enhance material functionality [101–105]. By implementing elemental doping strategies (e.g., rare earth ion implantation or transition metal substitution) as well as controllable defect construction (including vacancy defects and dislocation modulation, etc.), researchers are able to achieve precise modulation of material properties [106–109]. Taking GaN-based compounds and wide bandgap oxide systems in third-generation semiconductor materials as an example, advanced defect engineering design not only significantly improves carrier mobility (1000–1500 cm^2·V^{-1}·s^{-1}) and breakdown field strength (>3 MV·cm^{-1}), but also realizes linear enhancement of photoelectric response in the visible-ultraviolet region (about 40% increase in external quantum efficiency (EQE)) through defect energy level modulation [110–112]. Recent advances in defect stabilization mechanisms further expand the scope of defect engineering. Ivády et al. demonstrated that quantum wells formed by Frank-type stacking faults in 4H-SiC can stabilize divacancy spin qubits by locally lowering the conduction band minimum (~0.24 eV reduction) through polytypic 6H-SiC inclusions (Fig. 9). This quantum confinement effect enables selective ionization of divacancy dark states (VV^-) under optical excitation, significantly enhancing charge state stability during room-temperature spin manipulation [113]. Such crystallographically engineered environments provide a materials-centric solution to persistent challenges in photoionization-induced charge fluctuations. In addition, recent advances in 2D van der Waals semiconductors, such as CrSCl with intrinsic p-type conductivity and multipolarity coexistence, further demonstrate the potential of defect engineering beyond conventional doping paradigms [114]. This micro-regulation technology has been successfully applied to high-power electronic devices, deep-ultraviolet LEDs, photovoltaic catalysis and other cutting-edge fields, and the industrialization conversion rate of relevant research results has been increased by nearly 70% compared with the traditional process, promoting the continuous development of wide bandgap semiconductor materials toward high integration and low energy consumption.

Along this technological path, diamond, as a typical wide-band semiconductor material, shows significant advantages in the field of miniaturization of high-power electronic devices by virtue of its ultra-high breakdown field strength (>10 MV·cm^{-1}) and excellent carrier mobility (≥2000 cm^2·V^{-1}·s^{-1}) [115]. Although significant progress has been made in boron-doped p-type diamond (BDD), efficient n-type doping is still a key technological bottleneck limiting the development of diamond devices due to the high dissociation energy property of the donor impurity. To address

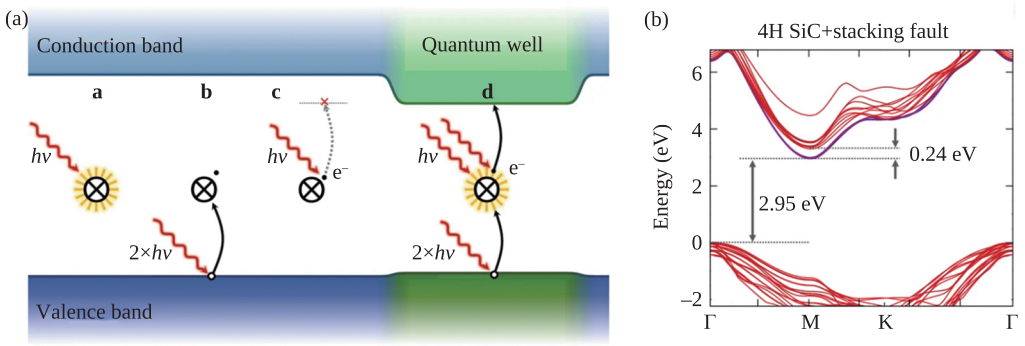

Figure 9 Comparison of light-state and dark-state dynamical mechanisms of quantum systems under optical excitation and energy band structure of defective 4H-SiC containing layer faults. (a) Mechanisms of light and dark state dynamics of quantum systems under optical excitation. **a**. A bright state of a color center under optical excitation. **b.** These incident photons may ionize the defect and turn it into a dark state, while **c.** does not have sufficient energy to repopulate the bright state. **d.** In a quantum well, however, the excitation laser can successfully re-pump the bright state. (b) Band structure of a defective 4H-SiC including a stacking fault. Red curves depict bulk-like conduction and valence band states in the basal plane of the hexagonal Brillouin zone. Purple curves show the stacking fault states that localized in the *c* direction and are dispersive in the basal plane. Reproduced with permission from Ref. [113]. ©2019, Springer Nature.

this challenge, Liu's research team successfully prepared boron-rich layers of 1–1.5 μm thickness on the (111) crystal surface of boron-doped diamond single crystals using the temperature gradient growth (TGG) method [116]. This study shows that by precisely tuning the experimental parameters during diamond crystallization, the controllable formation of B-O complexes can be achieved, which in turn induces the material to exhibit n-type conducting properties. Mechanistic analysis based on first-principles calculations indicates that the B_3O and B_4O complexes form shallow donor energy levels in the diamond lattice, which is essentially responsible for the n-type semiconductor behavior. It is particularly noteworthy that the formation energies of these two complexes are as low as –4.27 eV and –6.05 eV, respectively, indicating their significant thermodynamic formation advantage in the diamond system. Further comparative analysis confirms that the B_4O complexes have the lowest formation energies compared to other defect configurations, thus dominating the crystal growth process. This study successfully breaks the technical bottleneck of n-type diamond preparation by innovatively introducing the doping strategy of B-O complexes, which provides a new research direction for the development of diamond-based semiconductor devices. This work not only elucidates the electronic structure regulation mechanism of the compound defects but also lays an important theoretical foundation for the subsequent performance optimization of diamond electronic devices.

Besides diamond, cubic boron nitride (c-BN) is another semiconductor material with great application potential. They serve as promising ultra-wideband semiconductors in the field of high-power, high-frequency electronics, and experimental measurements of their carrier mobility have long differed significantly. To elucidate the intrinsic physical mechanisms, Sanders's team systematically revealed the microscopic properties of carrier transport in these two types of materials and their governing laws for device performance through a first-principles approach [117]. In the study, density functional theory combined with many-body perturbation theory (G_0W_0 quasiparticle correction) was used to accurately calculate. It obtains the bandgap values of 5.66 eV and 6.80 eV for diamond and c-BN, respectively. It is found that the phonon-limited electron mobility at room temperature is similar for both materials (diamond: 1790 $cm^2 \cdot V^{-1} \cdot s^{-1}$, c-BN: 1610 $cm^2 \cdot V^{-1} \cdot s^{-1}$) by density functional perturbation theory using the maximally localized Wannier function method, but the hole mobility of c-BN (80.4 $cm^2 \cdot V^{-1} \cdot s^{-1}$) shows a two order of magnitude difference compared to that of diamond (1970 $cm^2 \cdot V^{-1} \cdot s^{-1}$). The phenomenon is attributed to the strong inelastic scattering effect induced by the significant increase in the effective mass of holes at the top of the c-BN valence band. The

study also reveals the dynamic evolution properties of the carrier scattering mechanism: lattice scattering dominates in the low temperature region, while neutral impurity scattering becomes the main constraint at high doping concentrations. The theoretical model predicts the n-type c-BN and p-type diamond mobility with an error of less than 20%, verifying the reliability of the computational framework. This work not only elucidates the competition mechanism between intrinsic scattering and defect scattering in ultra-wide bandwidth semiconductors but also points out that the inherent hole mobility defect of c-BN will seriously limit its application prospects in bipolar devices, providing theoretical guidance for material performance optimization.

The above systematically discusses the intrinsic properties of two types of typical wide-band semiconductor materials and reveals the regulatory mechanisms of doping and defect engineering on their energy band structures and carrier transport properties. In-depth analysis reveals that the key scientific issues that constrain the performance enhancement of these semiconductor devices focus on the precise analysis of defect behavior and the effective suppression of their harmful effects. Using hybridization density functional theory calculations, Gao et al. systematically investigated the local structural relaxation properties, formation energy evolution laws, and their electron migration properties of neutral/charged intrinsic point defects (including vacancy, interstitial, and antisite defects) in GaN, AlN, and InN crystal systems [118]. By comparing the jump energy levels associated with the Fermi energy levels, it is found that Ga interstitial, nitrogen vacancy, N interstitial, In antisite, and In interstitial in the GaN system are stable only in the positive charge state with a donor energy level. While In vacancy are more stable in the neutral state, the other defects show both donor and acceptor behavior. Theoretical analysis of defect states shows that nitrogen vacancy in p-type nitrides and gallium/aluminum vacancy in n-type nitrides are the most stable defect configurations, a finding that provides a microscopic explanation for self-compensating effects in nitride materials and elucidates the physical cause of defect-induced n/p-type doping efficiency decay. It is also confirmed that the diffusion rate of nitrogen interstitials is significantly higher than that of vacancy defects, which directly leads to the low concentration characteristic of nitrogen interstitials and nitrogen-based defect complexes in nitrides. It is particularly noteworthy that the trends of formation energies, jump energy levels, and migration barriers of nitrides show significant correlations with their intrinsic atomic sizes and the width of the bandgap. The theoretical framework for defect identification and control established in this work is of great importance in guiding the performance optimization and reliability enhancement of nitride semiconductor devices.

Doping and defect engineering play a critical role in the performance modulation of broadband semiconductor materials, the core of which lies in the precise modulation of energy band structure, carrier dynamics and defect behavior through atomic-scale design. Using diamond and cubic boron nitride (c-BN) as examples, the study reveals the intrinsic constraints on carrier mobility in ultrawide-bandgap semiconductors: Although diamond has excellent carrier transport properties, its n-type doping has long been limited by the high dissociation energy of the sizing impurity, and innovative doping strategies based on the B-O complexes provide a new way to break the bottleneck by constructing a shallow sizing energy level; while in c-BN, the significant increase in the effective mass of the hole leads to a significant increase in the effective mass of the hole. The significant increase in effective mass leads to a sharp decrease in hole mobility, highlighting the inherent defects of its bipolar device applications. In nitride semiconductors, the defect-induced self-compensation effect and the dynamic evolution characteristics further reveal the microscopic roots of the doping efficiency decay. Complementary studies on GaN systems highlight the tunability of defect-mediated properties. Liao et al. systematically investigated C_N point defects in GaN NWs, revealing their dual role in enhancing electrical conductivity (1.15×10^{14} $W\cdot m^{-1}\cdot K^{-1}$ at 700 K) while suppressing Seebeck coefficients (0.0008 $V\cdot K^{-1}$ at 700 K). As shown in Figs. 10(a) and 10(b), the increased density of states near the Fermi level from C(p)-N(p) orbital hybridization drives these effects, offering a trade-off strategy for optimizing thermoelectric

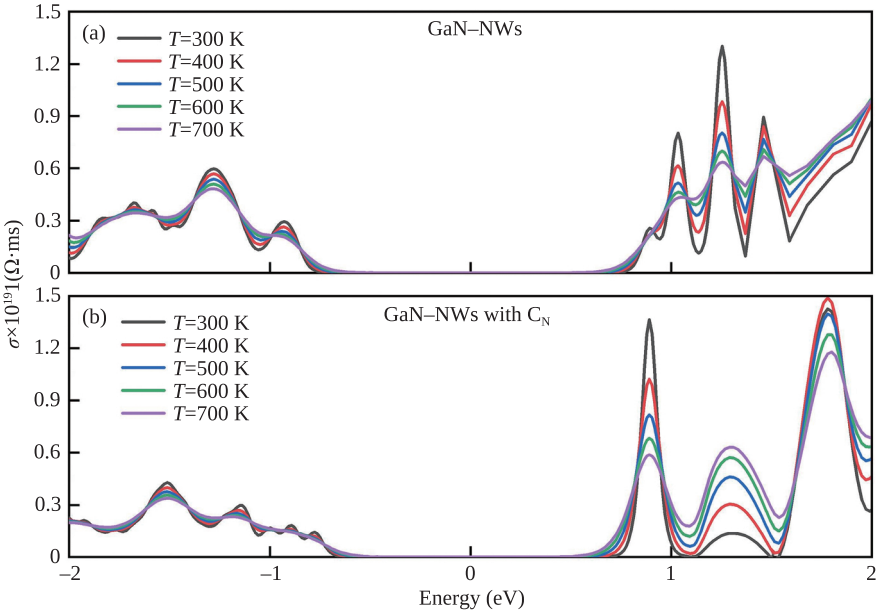

Figure 10 Changes in electrical conductivity of GaN NWs: (a) Intrinsic GaN NWs and (b) GaN NWs containing C_N point defects. Reproduced with permission from Ref. [119]. © 2023, Elsevier.

performance [119]. Theoretical calculations based on the ab initio methods have deeply resolved the correlation mechanism between defect formation energy and electronic structure, providing an important theoretical basis for suppressing harmful defects and optimizing doping paths. Taken together, these studies show that the synergistic design of atomic-level defect engineering and energy-band engineering, which reconciles the contradiction between intrinsic material properties and doping regulation, is the key way to advance wide bandgap semiconductors toward high-performance and high-reliability devices.

3 Application of first-principles calculations to the design of wide bandgap semiconductor devices

As materials science enters the era of "atomic engineering", the quantum correlation between microscopic electronic structures and their macroscopic properties has become the key to overcoming technical bottlenecks. The traditional experience-driven materials research and development model is limited by high costs and a long trial-and-error cycle, making it difficult to meet the urgent demand for high-performance materials in strategic fields such as clean energy and quantum information. In this context, first-principles calculations, which are based on the fundamental laws of quantum mechanics and require no empirical parameters, are reshaping the theoretical framework and practical ways of materials design. By solving the many-body Schrödinger equation, the method can accurately analyze the intrinsic physical properties of materials (e.g., energy band topology, defect dynamics, interfacial charge transport, etc.) and provide atomic-scale insights into key issues such as predicting cell electrode mobility barriers, chalcogenide defect suppression, and Schottky junctions [120–122]. With the innovation of density functional theory algorithms and the leap of supercomputing technology, its application boundary has been expanded from static physical property calculations to dynamic multiscale modeling, and through deep fusion with molecular dynamics, machine learning, and high-throughput screening, it achieves a cross-level breakthrough from predicting single-atom catalytic activity to simulating mesoscopic device performance.

In recent decades, new nanostructured materials, represented by diamond, β-SiCN, SiCN, GaN, metal oxides, and metal sulfides, have been developed into a new generation of broadband semiconductor systems that show remarkable potential as high-performance UV photodetectors [123, 124]. Interestingly, the successful synthesis of fully deprotected tetraethynylsilane

$(Si(C{\equiv}CH)_4)$ and its silicon derivatives reveals special electronic structural features: both its highest occupied molecular orbital (HOMO) and its lowest unoccupied molecular orbital (LUMO) exhibit triplet simplicity. Theoretical analysis shows that there is a significant Si-d orbital hybridization with C≡C group π* orbitals in the LUMO orbitals of this material, and this unique d-π* bonding synergistic effect provides a structural basis for the construction of multifunctional optoelectronic devices. On this basis, Sun et al. constructed diamond-like SiC_4 semiconductors by biomimetic design and systematically revealed their physical properties and potential applications [125]. Molecular dynamics simulations show that SiC_4 remains stable in the pair correlation functions $g(r)$ at 1500 K, while the characteristic peak at about 8 Å does not disappear until the temperature is increased to 2000 K, confirming the excellent high-temperature thermal stability of the material. This provides important support for device applications in extreme environments. The calculation of the optical absorption spectrum shows that the material exhibits significant absorption properties in the 100–300 nm UV band, with the main absorption peaks located near 100 nm and 250 nm, respectively, a feature highly compatible with its applicability as a UV photodetection material. In terms of mechanical properties, diamond-like SiC_4 has a lattice parameter of 7.857 Å, a density of only 0.74 g/cm³ (less than that of water), and a Young's modulus that is significantly smaller than that of diamond and single-crystal silicon. In particular, its Poisson's ratio reaches 0.476, close to the theoretical limit of 0.5, which is significantly higher than that of conventional silicon-based materials, indicating that the material has the mechanical properties of ultra-light weight, high flexibility, and resistance to compressive deformation. This study predicts a new semiconductor material with both wide bandgap properties, solar blind UV absorption, and high photoresponse efficiency with low dark current through theoretical calculations. Its unique synergistic optimization of thermal stability and mechanical properties provides an important material candidate system for the development of a new generation of flexible optoelectronic devices.

In addition to traditional three-dimensional semiconductor material systems, two-dimensional (2D) materials are attracting attention for their unique advantages in sensors, catalysts, and energy storage/conversion devices [126, 127]. In the exploration of new two-dimensional semiconductor materials, the anisotropic electron transport property opens a new avenue for the directional design of nanodevices. Jiang et al. show, based on first-principles calculations, that the new two-dimensional material InTe has an extraordinary electron mobility: its x-direction electron mobility reaches 12,137.80 $cm^2{\cdot}V^{-1}{\cdot}s^{-1}$, while the y-direction is only 13.79 $cm^2{\cdot}V^{-1}{\cdot}s^{-1}$) (Table 1) [128]. This remarkable mobility anisotropy gives InTe monolayers an advantage in nanoelectronic devices. Combined with an intrinsic bandgap of 2.735 eV, the material is particularly suitable for the construction of directional carrier transport channels in low-power,

Table 1 Calculated effective mass (m^*), and mobility (μ) of electrons and holes at x- and y- directions at 300 K for the InTeI monolayer and multilayers [128].

Carrier type	N_L	m^*x/m_0	m^*y/m_0	μ_x ($cm^2{\cdot}V^{-1}{\cdot}s^{-1}$)	μ_y ($cm^2{\cdot}V^{-1}{\cdot}s^{-1}$)
Electron	1L	1.65	0.84	12 137.80	13.79
	2L	1.42	0.35	4 116.76	133.24
	3L	0.81	0.34	382.01	391.34
	4L	0.76	0.29	703.31	766.75
	5L	0.69	0.24	1 473.84	1 389.55
Hole	1L	2.96	0.75	60.70	42.45
	2L	2.76	1.53	69.54	17.65
	3L	2.47	1.05	37.34	221.26
	4L	2.01	1.00	16.08	801.84
	5L	2.02	1.06	93.25	794.92

high-frequency electronic devices. In particular, its low exfoliation energy of 0.21 J/m^2 (only 52.5% of that of phosphene monolayers) provides a theoretical basis for realizing mechanical exfoliation preparation of high-quality 2D structures, avoiding the defect problems associated with complex chemical vapor deposition processes. Through systematic strain engineering simulations, this work reveals a unique energy band modulation law for InTe monolayers: the application of uniaxial strain induces a transition of the material from an indirect to a direct bandgap. This tunable electronic structure shows potential for applications in strain sensors and tunable optoelectronic devices. When extended to a multilayer structure, theoretical calculations show that the energy bands of InTe form a quasi-direct bandgap feature near the gamma point, and this layer-dependent energy band evolution law provides a new design dimension for the design of novel stacked photodetectors. To address the environmental stability of 2D materials, the ab initio molecular dynamics (AIMD) simulations of this work found that no dissociation reaction occurred when gas-phase O_2 interacted with InTe monolayers at room temperature, and the O_2 dissociation energy barrier was calculated to be 0. The O_2 dissociation energy barrier was calculated to be 0. 69 eV by the climbing image nudged elastic band (CI-NEB) method, and its antioxidant performance is between that of black phosphazene (0.31 eV) and α-P_3Cl_2 monolayer (1.14 eV), confirming that the material has the required environmental stability for practical application. Notably, symmetry engineering strategies in 2D transition metal systems have enabled reconfigurable p- and n-type FETs through structural modulation, highlighting the critical role of crystal symmetry in carrier transport optimization [129]. Further, recent advances further extend 2D materials to mid-infrared optoelectronics. Yu et al. demonstrated that bilayer $PtSe_2$ with controlled Se vacancies exhibits a tunable bandgap down to 0.3 eV (Fig. 11), enabling broadband photodetection from visible (632 nm) to mid-infrared (10 μm) with responsivity up to 4.5 A·W^{-1} [130]. This defect engineering strategy, combined with the layer-dependent quantum confinement effect, highlights the potential of 2D noble metal dichalcogenides to overcome the traditional limitations of III–V and IV–VI semiconductors in long-wavelength photonic integration.

Low-dimensional material systems (including two-dimensional, one-dimensional, and zero-dimensional systems), as a frontier field of condensed matter physics and materials science, have attracted much attention due to their unique physical properties and potential for applications in microelectronic devices. Among them, one-dimensional materials have become an important platform for the design of functional materials due to their highly exposed active sites, significant aspect ratio features, and the advantages of mechanical property modulation under dimensional constraints. Based on this, Shen et al. present a novel one-dimensional $PdGeS_3$ nanocrystalline chain system through first-principles calculations, which shows multidimensional applications. Theoretical calculations show that the exfoliation energy of the material is 105 meV/atom, which is lower than the solvation threshold for typical layered materials, confirming that it can be prepared in a controlled manner by the mechanical exfoliation method [131]. Phonon spectral analysis, together with AIMD simulation results, confirms the excellent

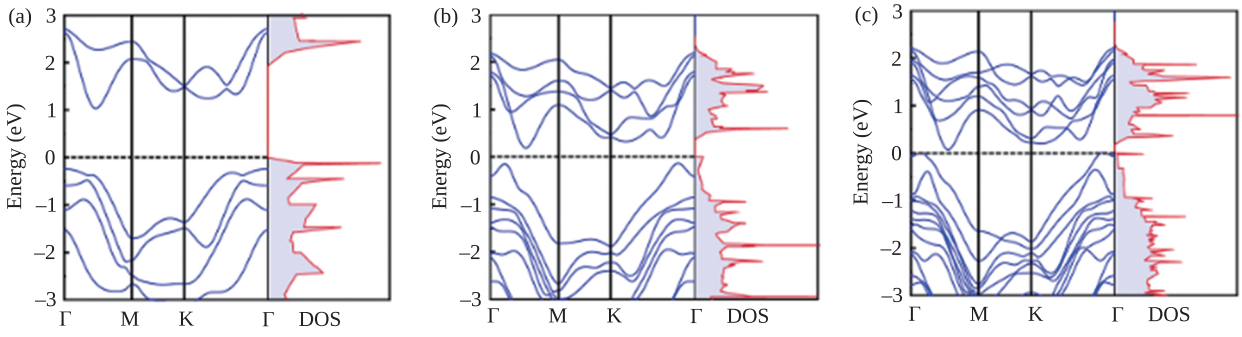

Figure 11 Characterization of atomically thin $PtSe_2$ and the bandgap evolution obtained by first-principles calculations (a), bilayer (b), and trilayer $PtSe_2$ (c) by first-principles calculations. Reproduced with permission from Ref. [130]. © 2018, Elsevier.

kinetic stability of the one-dimensional $PdGeS_3$ nanocrystalline chains at room temperature. Electronic structure calculations show that the material is an indirect bandgap semiconductor with a bandgap value of 2.86 eV based on the HSE06 generalized correction and that effective modulation of the bandgap value can be achieved by strain engineering. Notably, its electron mobility reaches 1506 $cm^2 \cdot V^{-1} \cdot s^{-1}$, which is 1–2 orders of magnitude higher than most of the reported one-dimensional materials and some two-dimensional systems, while the hole mobility is only 18 $cm^2 \cdot V^{-1} \cdot s^{-1}$ (Table 2). This significant difference in carrier mobility is conducive to the realization of highly efficient charge separation, which exhibits a unique advantage in the photocatalytic field. Light absorption characterization shows that both single and multi-chain $PdGeS_3$ exhibit strong absorption in the ultraviolet band with absorption coefficients in the order of 10^5 cm^{-1}, which is highly compatible with their potential applications in field-effect transistors and photodetectors. Through the synergistic application of multi-scale first-principle computational methods, this study has constructed a complete theoretical framework from structural stability, electronic properties, to photoresponse behavior, which fully demonstrates the important role of computational material science in the design and performance prediction of new low-dimensional materials.

In the design of wide-bandgap semiconductor devices, material selection is crucial. As the core foundation of device design, material selection requires accurate calculation of intrinsic physical parameters such as electronic energy band structure, carrier mobility, dielectric function, etc., to evaluate their technical applicability scientifically. The first-principles calculations based on density functional theory can effectively regulate key parameters such as forbidden bandwidth, carrier concentration, and lattice thermal conductivity of materials, providing theoretical guidance for material system optimization. Recent computational studies have expanded the horizon of unconventional wide-gap semiconductors. For instance, $Mg(OH)_2$—traditionally considered an insulator with a 5.7 eV bandgap—exhibits tunable conductivity through impurity engineering. First-principles calculations reveal that trivalent substitutional dopants (e.g., Al, Fe) introduce shallow donor states near the conduction band, while interlayer F atoms act as shallow acceptors by creating hole states close to the valence band maximum (Fig. 12) [132]. This dual doping mechanism demonstrates the feasibility of converting insulating hydroxides into functional semiconductors through defect control. In the field of optoelectronic device design, the DFT method can accurately predict optical parameters such as exciton binding energy, optical absorption coefficient, and quantum efficiency of materials, and reveal the structure-efficiency relationship between the microelectronic structure of materials and the macro-optoelectronic performance. For device structure optimization, the key factors such as interfacial state density, defect formation energy, and carrier transport path can be systematically investigated by constructing an atomic precision computational model, so as to establish a theoretical optimization framework for device structure design. In addition, this technology can effectively simulate the thermal transport behavior during device operation and guide the optimal design of the thermal management system through phonon spectrum analysis and lattice vibrational mode calculation. Finally, the overall performance of the device is subject to the synergistic effect of multiple physical mechanisms: microscopic processes such as carrier compound dynamics, interfacial energy band matching, and the point defect evolution law all have a significant impact on the macroscopic properties of the device. First-principles calculations can deeply analyze the interaction law of the above complex physical mechanisms by establishing a multi-scale correlation model. It is worth mentioning that this method can also

Table 2 Calculated effective mass ($|m^*|$), and carrier mobility (μ) of the electron and hole along the chain-directions at 300 K for the 1D $PdGeS_3$ nanochain [131].

System	Carrier	$\|m^*\|$ (m_0)	μ ($cm^2 \cdot V^{-1} \cdot s^{-1}$)
1D $PdGeS_3$	Hole	3.88	18
	Electron	0.53	1506

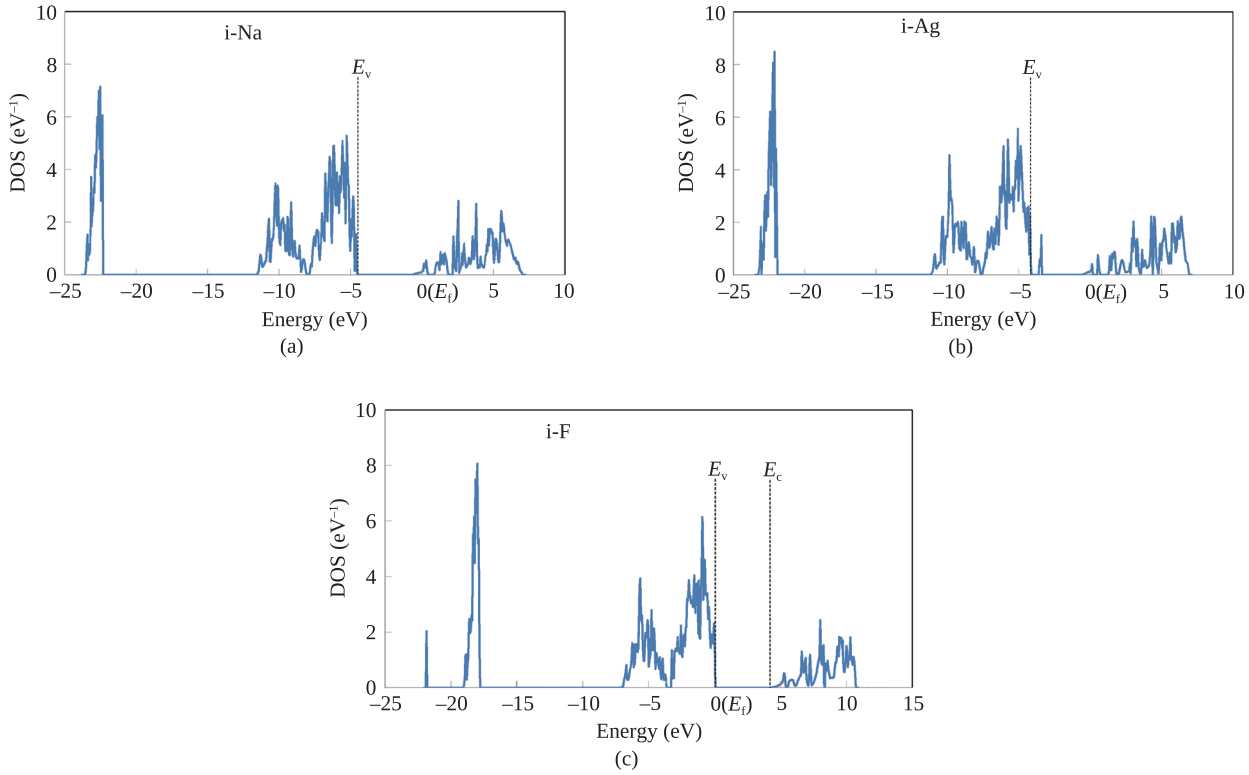

Figure 12 DOS of $Mg(OH)_2$ with an interlayer impurity: (a) Na, (b) Ag, and (c) F. Reproduced with permission from Ref. [132]. © 2021, Frontiers.

simulate the structural degradation of materials under continuous operation conditions, predict the failure mechanisms such as oxygen vacancy migration and surface reconstruction, and provide a prospective theoretical basis for device reliability research. Through the above discussion, it is not difficult to obtain that the application of first-principles calculations in the design of wide bandgap semiconductor devices has covered a variety of aspects, such as material selection, structure optimization, performance prediction, etc., and has provided theoretical support for the efficient and stable operation of the devices. With the continuous development of new technologies and methods, future research will pay more attention to the combination of computation and experiment, as well as the application of new computational methods. These innovations will promote the further development of wide bandgap semiconductor device design and open up new research areas and application directions.

4 Conclusion and outlook

First-principles calculations, as a core tool for revealing the physical nature of wide bandgap semiconductors, have gradually evolved from static physical property analysis to a comprehensive research paradigm of dynamic multiscale simulations. Through the synergistic application of density functional theory, multibody perturbation theory, and the Bethe-Salpeter equation, researchers have successfully achieved theoretical breakthroughs ranging from the precise modification of electronic structure, the quantitative analysis of exciton effects, and the cross-scale correlation of thermal transport behavior. In the field of defect engineering, the doping strategy based on the calculation of formation energy and migration barrier not only solves the problem of low efficiency of traditional n-type doping but also promotes the breakdown field strength to break through the 10 MV·cm^{-1} performance limit. In addition, the machine learning-learning high-throughput screening technology has greatly accelerated the discovery process of novel semiconductor materials, while the low-dimensional material design based on the first-principles calculations has revealed a new mechanism of anisotropic carrier transport, which provides an entirely new degree of freedom for the design

of nanoelectronic devices.

However, the field still faces serious challenges. On the one hand, the limitation of computational resources has become a bottleneck that limits the accurate simulation of large-scale systems. Although hardware advances have significantly improved computational efficiency, how to balance computational accuracy and scale is still the core contradiction when dealing with complex electronic interaction systems. Second, the multi-scale correlation mechanism between defects and interface effects has not been fully elucidated. Although existing methods can simulate the behavior of a single defect, there are still limitations in describing the dynamic evolution of defect clusters, interfacial charge redistribution, and other complex processes, leading to systematic deviations between theoretical predictions and experimental observations. Third, cross-scale modeling of coupled optical-electrical-thermal multi-physical fields lacks a universal framework, making it difficult to meet the demand for accurate prediction of device performance under extreme conditions. Based on the above discussion, future research needs to achieve a triple breakthrough at the methodological level:

(1) Develop efficient computational strategies enhanced by machine learning and optimize the high-throughput screening process by active learning and migration learning.

(2) Establish a defect-interface co-evolutionary model by combining non-equilibrium Green's function and real-time time-integrated density flooding theory to reveal the temporal and spatial evolution of defect dynamics.

(3) To construct a cross-scale computational framework for multi-physics field coupling, integrating electron-phonon interaction and non-adiabatic effects to realize a full working condition simulation of device operation behavior.

It is expected that with the development of exascale supercomputing and quantum-classical hybrid computing architectures, first-principles calculations will break through the simulation limit of the multi-million atom system, and ultimately establish a cross-scale correlation model from micro-defect regulation to macroscopic device performance, which will provide theoretical cornerstones and design guides for the revolution of wide-bandgap semiconductor technology.

Acknowledgments

We gratefully acknowledge the financial support received from the National Natural Science Foundation of China (Nos. 12474014, 62304069, 12104352, and 12204294), along with additional funding from the Natural Science Foundation of Jiangsu Province (No. BK20241843) and the Natural Science Basic Research Program of Shaanxi Province (No. 2023JC-X1-01). This work was also supported by the China National Postdoctoral Program for Innovative Talents (No. BX20230281), the China Postdoctoral Science Foundation (No. 2024M752520), and Xidian University's Interdisciplinary Exploration Special Fund (No. TZJH2024064).

References

[1] Y. Zhang, D. Dong, Q. Li, R. Zhang, F. Udrea, and H. Wang, "Wide-bandgap semiconductors and power electronics as pathways to carbon neutrality," *Nature Reviews Electrical Engineering*, vol. 2, pp. 155–172, 2025.

[2] J. Yang, K. Liu, X. Chen, and D. Shen, "Recent advances in optoelectronic and microelectronic devices based on ultrawide-bandgap semiconductors," *Progress in Quantum Electronics*, vol. 83, p. 100397, 2022.

[3] M. Zhang and Y. Zhang, "Status and prospects of wide bandgap semiconductor devices," *Applied and Computational Engineering*, vol. 23, pp. 252–262, 2023.

[4] S. Singh, T. Chaudhary, and G. Khanna, "Recent advancements in wide band semiconductors (SiC and GaN) technology for future devices," *Silicon*, vol. 14, no. 11, pp. 5793–5800, 2022.

[5] S. Sun, Y. Zhang, Y. Si, J. Xiong, and X. Luo, "Improvement of breakdown characteristic for a novel GaN HEMT with enhanced resistance single-event transient effect," *Journal of Electronic Materials*, vol. 54, no. 1, pp. 784–791, 2025.

[6] K. Woo, Z. Bian, M. Noshin, R. Perez Martinez, M. Malakoutian, B. Shankar, and S. Chowdhury, "From wide to ultrawide-bandgap semiconductors for high power and high frequency electronic devices," *Journal of Physics: Materials*, vol. 7, no. 2, p. 022003, 2024.

[7] J. Shi, "A deep dive into SiC and GaN power devices: Advances and prospects," *Applied and Computational Engineering*, vol. 23, no. 1, pp. 230–237, 2023.

[8] X. Sun, C. Zhang, J. Chang, H. Yang, H. Xi, G. Lu, D. Chen,

Z. Lin, X. Lu, and J. Zhang, "Mixed-solvent-vapor annealing of perovskite for photovoltaic device efficiency enhancement," *Nano Energy*, vol. 28, pp. 417–425, 2016.

[9] Y Hao, "New advances in broadband and ultra-broadband semiconductor devices," *Science & Technology Review*, vol. 37, no. 3, 2019.

[10] M. H. Wong, O. Bierwagen, R. J. Kaplar, and H. Umezawa, "Ultrawide-bandgap semiconductors: An overview," *Journal of Materials Research*, vol. 36, no. 23, pp. 4601–4615, 2021.

[11] M. Xiao, X. Duan, J. Zhang, and Y. Hao, "Enhancement-mode AlN/GaN HEMTs with high *I* on/*I* off and low-leakage-current fabricated with low-power surface oxidation treatment," *IEEE Electron Device Letters*, vol. 39, no. 5, pp. 719–722, 2018.

[12] O. S. Chaudhary, M. Denaï, S. S. Refaat, and G. Pissanidis, "Technology and applications of wide bandgap semiconductor materials: Current state and future trends," *Energies*, vol. 16, no. 18, p. 6689, 2023.

[13] M. Buffolo, D. Favero, A. Marcuzzi, C. De Santi, G. Meneghesso, E. Zanoni, and M. Meneghini, "Review and outlook on GaN and SiC power devices: Industrial state-of-the-art, applications, and perspectives," *IEEE Transactions on Electron Devices*, vol. 71, no. 3, pp. 1344–13552024.

[14] L. H. Thomas, "The calculation of atomic fields," *Mathematical Proceedings of the Cambridge Philosophical Society*, vol. 23, no. 5, pp. 542–548, 1927.

[15] D. R. Hartree, "The wave mechanics of an atom with a non-Coulomb central field. Part I. Theory and methods," *Mathematical Proceedings of the Cambridge Philosophical Society*, vol. 24, no. 1, pp. 89–110, 1928.

[16] P. Hohenberg and W. Kohn, "Inhomogeneous electron gas," *Physical Review*, vol. 136, no. 3B, p. B864, 1964.

[17] W. Kohn and L. J. Sham, "Self-consistent equations including exchange and correlation effects," *Physical Review*, vol. 140, no. 4A, p. A1133, 1965.

[18] R. Car and M. Parrinello, "Unified approach for molecular dynamics and density-functional theory," *Physical Review Letters*, vol. 55, no. 22, p. 2471, 1985.

[19] J. Zhou, G. Han, Q. Li, Y. Peng, X. Lu, C. Zhang, J. Zhang, Q.-Q. Sun, D. W. Zhang, and Y. Hao, "Ferroelectric $HfZrO_x$ Ge and GeSn PMOSFETs with Sub-60 mV/decade subthreshold swing, negligible hysteresis, and improved Ids," 2016 IEEE International Electron Devices Meeting (IEDM), San Francisco, CA, USA, 03–07 December 2016, pp. 12.12.11–12.12.14.

[20] S. X. Tao, X. Cao, and P. A. Bobbert, "Accurate and efficient band gap predictions of metal halide perovskites using the DFT-1/2 method: GW accuracy with DFT expense," *Scientific Reports*, vol. 7, no. 1, p. 14386, 2017.

[21] M. S. Hybertsen and S. G. Louie, "Electron correlation in semiconductors and insulators: Band gaps and quasiparticle energies," *Physical Review B*, vol. 34, no. 8, p. 5390, 1986.

[22] M. Shishkin and G. Kresse, "Self-consistent GW calculations for semiconductors and insulators," *Physical Review B*, vol. 75, no. 23, p. 235102, 2007.

[23] A. Shokri, Y. Melikhov, Y. Syryanyy, and I. N. Demchenko, "Point defects in silicon-doped β-Ga_2O_3: hybrid-DFT calculations," *ACS Omega*, vol. 8, no. 46, pp. 43732–43738, 2023.

[24] B. Ryu, E. -A. Choi, S. Park, J. Chung, J. de Boor, P. Ziolkowski, E. Müller, and S. Park, "Native point defects and low p-doping efficiency in Mg_2(Si, Sn) solid solutions: A hybrid-density functional study," *Journal of Alloys and Compounds*, vol. 853, p. 157145, 2021.

[25] M. Nishiwaki and H. Fujiwara, "Highly accurate prediction of material optical properties based on density functional theory," *Computational Materials Science*, vol. 172, p. 109315, 2020.

[26] M. A. Islam, N. Hossain, Z. Ahsan, M. Rana, M. Rahman, and M. Abdullah, "DFT insights into the mechanical properties of NMs," *Results in Surfaces and Interfaces*, vol. 18, p. 100417, 2025.

[27] Z. Li and A. Yin, "First-principles calculations of the Elastic properties, electronic structure and optical properties of hexagonal Al_4SiC_4," *Academic Journal of Science and Technology*, vol. 10, no. 1, pp. 181–185, 2024.

[28] T. Yang, C. Yan, S. Qiu, Y. Tang, A. Du, and J. Cai, "First-principles study of Penta-PtXY (X= Se, Te; Y= S, Te; X ≠ Y) monolayer with highly anisotropic electronic and optical properties," *ACS Omega*, vol. 9, no. 30, pp. 32502–32512, 2024.

[29] W. Gao, F. H. da Jornada, M. Del Ben, J. Deslippe, S. G. Louie, and J. R. Chelikowsky, "Quasiparticle energies and optical excitations of 3C-SiC divacancy from GW and GW plus Bethe-Salpeter equation calculations," *Physical Review Materials*, vol. 6, no. 3, p. 036201, 2022.

[30] K. Demmouche and J. Coutinho, "Electronic exchange-correlation, many-body effect issues on first-principles calculations of bulk SiC polytypes," *International Journal of Modern Physics B*, vol. 32, no. 29, p. 1850328, 2018.

[31] J. Lei, D. -P. Zhu, M. -C. Xu, and S. -J. Hu, "First-principles simulations of two dimensional electron gas near the interface of ZnO/GaN (0001) superlattice," *Physics Letters A*, vol. 379, no. 38, pp. 2384–2387, 2015.

[32] V. S. Olsen, G. Baldissera, C. Zimmermann, C. S. Granerød, C. Bazioti, A. Galeckas, B. G. Svensson, A. Y. Kuznetsov, C. Persson, and Ø. Prytz, "Evidence of defect band mechanism responsible for band gap evolution in $(ZnO)_{1-x}$ $(GaN)_x$ alloys," *Physical Review B*, vol. 100, no. 16, p. 165201, 2019.

[33] F. Aryasetiawan and O. Gunnarsson, "The GW method," *Reports on Progress in Physics*, vol. 61, no. 3, p. 237, 1998.

[34] A. L. Fetter and J. D. Walecka, *Quantum theory of many-particle systems*, Courier Corporation, 2012.

[35] W. G. Aulbur, L. Jönsson, and J. W. Wilkins, "Quasiparticle calculations in solids," *Solid State Physics*, vol. 54, pp. 1–218, 2000.

[36] L. Hedin, "New method for calculating the one-particle Green's function with application to the electron-gas problem," *Physical Review*, vol. 139, no. 3A, pp. A796–A823, 1965.

[37] L. Hedin and S. Lundqvist, "Effects of electron-electron and electron-phonon interactions on the one-electron states of solids," in *Solid State Physics*, Elsevier, 1970, pp. 1–181.

[38] H. Jiang, R. I. Gomez-Abal, P. Rinke, and M. Scheffler, "First-principles modeling of localized d states with the GW@LDA+U approach," *Physical Review B*, vol. 82, no. 4, p. 045108, 2010.

[39] M. S. Hybertsen and S. G. Louie, "Electron correlation in semiconductors and insulators: Band gaps and quasiparticle energies," *Physical Review B*, vol. 34, no. 8, pp. 5390–5413, 1986.

[40] V. S. Olsen, G. Baldissera, C. Zimmermann, C. S. Granerød, C. Bazioti, A. Galeckas, B. G. Svensson, A. Y. Kuznetsov, C. Persson, and Ø. Prytz, "Evidence of defect band mechanism responsible for band gap evolution in $(ZnO)_{1-x}(GaN)_x$ alloys," *Physical Review B*, vol. 100, no. 16, p. 165201, 2019.

[41] P. Rinke, M. Winkelnkemper, A. Qteish, D. Bimberg, J. Neugebauer, and M. Scheffler, "Consistent set of band parameters for the group-III nitrides AlN, GaN, and InN," *Physical Review B*, vol. 77, no. 7, p. 075202, 2008.

[42] C. Lee, N. D. Rock, A. Islam, M. A. Scarpulla, and E. Ertekin, "Electron–phonon effects and temperature-dependence of the electronic structure of monoclinic β-Ga_2O_3," *APL Materials*, vol. 11, no. 1, 2023.

[43] M.-Y. Zhang and H. Jiang, "Density-functional theory methods for electronic band structure properties of materials," *Scientia Sinica Chimica*, vol. 50, no. 10, pp. 1344–1362, 2020.

[44] D. M. Bylander and L. Kleinman, "Good semiconductor band gaps with a modified local-density approximation," *Physical Review B*, vol. 41, no. 11, pp. 7868–7871, 1990.

[45] A. Seidl, A. Görling, P. Vogl, J. A. Majewski, and M. Levy, "Generalized Kohn-Sham schemes and the band-gap problem," *Physical Review B*, vol. 53, no. 7, pp. 3764–3774, 1996.

[46] C. Zhang, J. Chen, J. Li, Y. Peng, and Z. Mao, "Large language models for human–robot interaction: A review," *Biomimetic Intelligence and Robotics*, vol. 3, no. 4, p. 100131, 2023.

[47] Y. Xu, X. Wang, X. Li, L. Xi, J. Ni, W. Zhu, W. Zhang, and J. Yang, "New materials band gap prediction based on the high-throughput calculation and the machine learning," *Scientia Sinica Technologica*, vol. 49, no. 1, pp. 44–54, 2019.

[48] Z. Chen, J. Wang, C. Li, B. Liu, D. Luo, Y. Min, N. Fu, and Q. Xue, "Highly versatile and accurate machine learning methods for predicting perovskite properties," *Journal of Materials Chemistry C*, vol. 12, no. 38, pp. 15444–15453, 2024.

[49] B. Sa, R. Hu, Z. Zheng, R. Xiong, Y. Zhang, C. Wen, J. Zhou, and Z. Sun, "High-Throughput computational screening and machine learning modeling of janus 2D III–VI van der waals heterostructures for solar energy applications," *Chemistry of Materials*, vol. 34, no. 15, pp. 6687–6701, 2022.

[50] H. Shen, J. Wu, Z. Chen, X. Fang, J. Li, W. Li, J. Lin, F. Zhu, X. Wang, and Y. Chen, "First-principles study combined with interpretable machine-learning models of bayesian optimization for the design of ultrawide bandgap double perovskites," *The Journal of Physical Chemistry C*, vol. 127, no. 43, pp. 21410–21422, 2023.

[51] N. Sharma, Y. Gupta, V. Kanungo, A. K. Sharma, and A. Sharma, "Survey of machine learning-augmented TCAD algorithms for modeling GaN HEMTs," in *Circuit Design for Modern Applications*, CRC Press, pp. 353–370,

[52] C. Zhu, J. Ni, Z. Yang, Y. Sheng, J. Yang, and W. Zhang, "Bandgap prediction on small thermoelectric material dataset via instance-based transfer learning," *Computational and Theoretical Chemistry*, vol. 1217, p. 113872, 2022.

[53] X. Tian, S. Zhou, H. Hao, H. Ruan, R. R. Gaddam, R. C. Dutta, T. Zhu, H. Wang, B. Wu, N. P. Brandon et al., "Machine learning and density functional theory for catalyst and process design in hydrogen production," *Chain*, vol. 1, no. 2, pp. 150–166, 2024.

[54] Z. Mao, Y. Peng, C. Hu, R. Ding, Y. Yamada, and S. Maeda, "Soft computing-based predictive modeling of flexible electrohydrodynamic pumps," *Biomimetic Intelligence and Robotics*, vol. 3, no. 3, p. 100114, 2023.

[55] C. Gu, W. Lin, X. He, L. Zhang, and M. Zhang, "IMU-based motion capture system for rehabilitation applications: A systematic review," *Biomimetic Intelligence and Robotics*, vol. 3, no. 2, p. 100097, 2023.

[56] X. Wang, H. Yu, S. Kold, O. Rahbek, and S. Bai, "Wearable sensors for activity monitoring and motion control: A review," *Biomimetic Intelligence and Robotics*, vol. 3, no. 1, p. 100089, 2023.

[57] T. Lei, T. Sellers, C. Luo, D. W. Carruth, and Z. Bi, "Graph-based robot optimal path planning with bio-inspired algorithms," *Biomimetic Intelligence and Robotics*, vol. 3, no. 3, p. 100119, 2023.

[58] M. S. Khan, L.-j. Shi, and B. Zou, "First principles calculations of optoelectronic and magnetic properties of Co-doped and (Co, Al) co-doped ZnO," *Journal of Applied Physics*, vol.

127, no. 6, p. 065707, 2020.

[59] D. Seiler, S. Zollner, A. Diebold, and P. Amirtharaj, "Optical properties of semiconductors," *Handbook of Optics*, McGraw Hill, New York, NY, 2009.

[60] M. Razeghi, "Optical properties of semiconductors," in *Fundamentals of Solid State Engineering*, Cham: Springer International Publishing, 2019, pp. 365–407.

[61] S. W. Koch, T. Meier, W. Hoyer, and M. Kira, "Theory of the optical properties of semiconductor nanostructures," *Physica E*, vol. 14, no. 1, pp. 45–52, 2002.

[62] A. E. Kourdaci, I. Bourachid, H. Bouafia, K. Mecheri, B. Abidri, and D. Rached, "First-principles calculations to examine structural, magnetic, mechanical, electronic and optical properties of wide bandgap semiconductor gadolinium aluminum oxide perovskite $GdAlO_3$," *Computational Condensed Matter*, vol. 38, p. e00889, 2024.

[63] Y. Duan and Y. Sun, "First-principles calculations of optical properties of Mg_2Pb," *Science China Physics, Mechanics and Astronomy*, vol. 57, no. 2, pp. 233–238, 2014.

[64] B. Peng, H. Zhang, H. Shao, Y. Xu, R. Zhang, and H. Zhu, "The electronic, optical, and thermodynamic properties of borophene from first-principles calculations," *Journal of Materials Chemistry C*, vol. 4, no. 16, pp. 3592–3598, 2016.

[65] J. Jiang, R. Pachter, and S. Mou, "Tunability in the optical response of defective monolayer WSe_2 by computational analysis," *Nanoscale*, vol. 10, no. 28, pp. 13751–13760, 2018.

[66] K. Gilmore, J. Vinson, E. L. Shirley, D. Prendergast, C. D. Pemmaraju, J. J. Kas, F. D. Vila, and J. J. Rehr, "Efficient implementation of core-excitation Bethe–Salpeter equation calculations," *Computer Physics Communications*, vol. 197, pp. 109–117, 2015.

[67] S. G. Louie and A. Rubio, "Quasiparticle and optical properties of solids and nanostructures: The GW-BSE approach," in *Handbook of Materials Modeling: Methods*, Springer, 2005, pp. 215–240.

[68] G. Strinati, "Application of the Green's functions method to the study of the optical properties of semiconductors," *La Rivista del Nuovo Cimento (1978-1999)*, vol. 11, no. 12, pp. 1–86, 1988.

[69] S. Albrecht, L. Reining, R. Del Sole, and G. Onida, "*Ab initio* calculation of excitonic effects in the optical spectra of semiconductors," *Physical Review Letters*, vol. 80, no. 20, pp. 4510–4513, 1998.

[70] M. Rohlfing and S. G. Louie, "Electron-hole excitations in semiconductors and insulators," *Physical Review Letters*, vol. 81, no. 11, pp. 2312–2315, 1998.

[71] C. Holzer, A. Pausch, and W. Klopper, "The GW/BSE method in magnetic fields," *Frontiers in Chemistry*, vol. 9, art. no. 746162, 2021.

[72] X. Leng, F. Jin, M. Wei, and Y. Ma, "GW method and Bethe–Salpeter equation for calculating electronic excitations," *Wiley Interdisciplinary Reviews: Computational Molecular Science*, vol. 6, no. 5, pp. 532–550, 2016.

[73] D. P. Gulo, N. Tuan Hung, W.-L. Chen, S. Wang, M. Liu, E. I. Kauppinen, H. Takehara, A. Taguchi, T. Taniguchi, and S. Maruyama, "Quenching of defect-induced photoluminescence in a boron-nitride and carbon hetero-nanotube," *The Journal of Physical Chemistry Letters*, vol. 16, pp. 1711–1719, 2025.

[74] J. Park and S.-M. Hong, "First principles calculation of band offsets and defect energy levels in Al_2O_3/β-Ga_2O_3 interface structures with point defects," *Journal of Semiconductor Technology and Science*, vol. 19, no. 4, pp. 413–425, 2019.

[75] A. Babu and N. M. Rao, "Effect of copper substitution on the structural, optical, and magnetic properties of β-Ga_2O_3 powders," *Applied Physics A*, vol. 131, no. 3, pp. 1–15, 2025.

[76] M. Fregolent, F. Piva, M. Buffolo, C. De Santi, A. Cester, M. Higashiwaki, G. Meneghesso, E. Zanoni, and M. Meneghini, "Advanced defect spectroscopy in wide bandgap semiconductors: Review and recent results," *Journal of Physics D: Applied Physics*, vol. 57, p. 433002, 2024.

[77] M. M. Krause and P. Kambhampati, "Linking surface chemistry to optical properties of semiconductor nanocrystals," *Physical Chemistry Chemical Physics*, vol. 17, no. 29, pp. 18882–18894, 2015.

[78] S. Feng, J. Liu, J. Chen, L. Su, F. Guo, C. Tang, C. Yuan, and X. Cheng, "First-principles study on electronic and optical properties of van der Waals heterostructures stacked by g-ZnO and Janus-WSSe monolayers," *Applied Surface Science*, vol. 604, p. 154620, 2022.

[79] L. Wu, D. Yang, Y. Dong, Z. Wang, Y. Zhang, T. Wang, L. Cheng, Y. Wang, and Y. Wu, "Enhanced CO_2 reduction via S-Scheme heterojunction of amorphous/crystalline metal-free carbon nitride photocatalysts," *Chemical Engineering Journal*, vol. 500, p. 156777, 2024.

[80] K. S. Novoselov, A. Mishchenko, A. Carvalho, and A. Castro Neto, "2D materials and van der Waals heterostructures," *Science*, vol. 353, no. 6298, p. aac9439, 2016.

[81] M. Jiang, D. Kong, M. Zhang, H. Lan, Q. Hu, Y. Zhou, and J. Zhou, "Advances in 2D materials for infrared photodetection: Synthesis, heterostructures, and device innovations," *Advanced Physics Research*, Early View, p. 2400199, 2025.

[82] P. V. Pham, S. C. Bodepudi, K. Shehzad, Y. Liu, Y. Xu, B. Yu, and X. Duan, "2D heterostructures for ubiquitous electronics and optoelectronics: Principles, opportunities, and challenges," *Chemical Reviews*, vol. 122, no. 6, pp. 6514–6613, 2022.

[83] D. Deng, K. Novoselov, Q. Fu, N. Zheng, Z. Tian, and X.

Bao, "Catalysis with two-dimensional materials and their heterostructures," *Nature Nanotechnology*, vol. 11, no. 3, pp. 218–230, 2016.

[84] S. He, Y. Zhang, H. Yao, H. Zuo, H. Wang, and G. Feng, "Effect of impurity distribution on optical properties of Cr-doped ZnSe nanowires: A first-principles study," *Results in Physics*, vol. 48, p. 106459, 2023.

[85] H. Mustafa, M. Irfan, A. Sattar, R. J. Amjad, H. Latif, A. Usman, M. Ashfaq Ahmad, and S. Qin, "First principle study of multilayered graphene/MoS_2 heterostructures for photodetectors," *Materials Science and Engineering B*, vol. 289, p. 116205, 2023.

[86] M. R. Islam, R. H. Galib, M. Sarkar, and S. Chowdhury, "Wide-bandgap semiconductor device technologies for high temperature and harsh environment applications," *Harsh Environment Electronics. Interconnect Materials and Performance Assessment*, Wiley Semiconductors, 2018.

[87] F. -F. Zeng, Q. -S. Zhang, S. -D. Zhang, Q. Sun, H. -T. Guo, Q. -Q. Xiao, Q. Xie, L. Zhang, G. -F. Fan, Y. -P. Qu et al., "Enhanced energy-storage performances and thermal stability in BNT–LST-based ceramics by tuning domain configuration and bandgap," *Rare Metals*, in press, 2025, doi 10.1007/s12598-024-03051-7.

[88] P. R. Chalker, "Wide bandgap semiconductor materials for high temperature electronics," *Thin Solid Films*, vol. 343–344, pp. 616–622, 1999.

[89] G. Alvarez-Escalante, R. Page, R. Hu, H. G. Xing, D. Jena, and Z. Tian, "High thermal conductivity and ultrahigh thermal boundary conductance of homoepitaxial AlN thin films," *APL Materials*, vol. 10, no. 1, p. 011115, 2022.

[90] X. L. Shi, J. Zou, and Z. G. Chen, "Advanced thermoelectric design: From materials and structures to devices," *Chemical Reviews*, vol. 120, no. 15, pp. 7399–7515, 2020.

[91] K. A. Peterson, E. M. Thomas, and M. L. Chabinyc, "Thermoelectric properties of semiconducting polymers," *Annual Review of Materials Research*, vol. 50, no. 1, pp. 551–574, 2020.

[92] Y. Song, X. Dai, Y. Zou, C. Li, C. -A. Di, D. Zhang, and D. Zhu, "Boosting the thermoelectric performance of the doped DPP-EDOT conjugated polymer by incorporating an ionic additive," *Small*, vol. 19, no. 29, p. 2300231, 2023.

[93] D. Wang, J. Ding, X. Dai, L. Xiang, D. Ye, Z. He, F. Zhang, S. H. Jung, J. K. Lee, and C. A. Di, "Triggering ZT to 0.40 by engineering orientation in one polymeric semiconductor," *Advanced Materials*, vol. 35, no. 2, p. 2208215, 2023.

[94] R. Jain, S. Jain, C. Nagarjuna, S. Samal, A. P. Rananavare, S. K. Dewangan, and B. Ahn, "A comprehensive review on hot deformation behavior of high-entropy alloys for high temperature applications," *Metals and Materials International*, online first, doi 10.1007/s12540-024-01888-2.

[95] P. Trocha, "Spin-dependent thermoelectric properties of a hybrid ferromagnetic metal/quantum dot/topological insulator junction," *Scientific Reports*, vol. 15, no. 1, p. 4904, 2025.

[96] G. Mahan and J. Sofo, "The best thermoelectric," *Proceedings of the National Academy of Sciences*, vol. 93, no. 15, pp. 7436–7439, 1996.

[97] S. Tang, M. Wu, S. Bai, D. Luo, J. Zhang, and S. Yang, "Honeycomb-like puckered PbTe monolayer: A promising n-type thermoelectric material with ultralow lattice thermal conductivity," *Journal of Alloys and Compounds*, vol. 907, p. 164439, 2022.

[98] G. Zhao, H.-P. Liang, and Y.-F. Duan, "Visible light modulation and anomalous thermal transport in two-dimensional X-AlN (X = C, Si, TC) semiconductor," *Acta Physica Sinica*, vol. 72, no. 9, p. 096301, 2023.

[99] F. Li, U. Aeberhard, H. Wu, M. Qiao, and Y. Li, "Global minimum beryllium hydride sheet with novel negative Poisson's ratio: First-principles calculations," *RSC advances*, vol. 8, no. 35, pp. 19432–19436, 2018.

[100] M. Zhao, X. Sun, P. Ji, T. Li, Y. Lu, L. Ma, C. Xu, S. Jiao, J. Dai, and Y. Wu, "Giant electrocaloric effect and breakdown field strength in ferroelectric terpolymer nanocomposites by morphologically diverse nanostructures," *Nano Energy*, vol. 128, p. 109948, 2024.

[101] S. Liu, S. Bai, Y. Wen, J. Lou, Y. Jiang, Y. Zhu, D. Liu, Y. Li, H. Shi, S. Liu et al., "Quadruple-band synglisis enables high thermoelectric efficiency in earth-abundant tin sulfide crystals," *Science*, vol. 387, no. 6730, pp. 202–208, 2025.

[102] C. Nie, C. Wang, Y. Xu, Y. Liu, X. Niu, S. Li, Y. Gong, Y. Hou, X. Zhang, D. Zhang et al., "Band modification and localized lattice engineering leads to high thermoelectric performance in Ge and Bi codoped SnTe–$AgBiTe_2$ alloys," *Small*, vol. 19, no. 28, p. 2301298, 2023.

[103] L. Wang, X. Tan, G. Liu, J. Xu, H. Shao, B. Yu, H. Jiang, S. Yue, and J. Jiang, "Manipulating band convergence and resonant state in thermoelectric material SnTe by Mn–In codoping," *ACS Energy Letters*, vol. 2, no. 5, pp. 1203–1207, 2017.

[104] C. Chang, Y. Liu, S. Ho Lee, M. Chiara Spadaro, K. M. Koskela, T. Kleinhanns, T. Costanzo, J. Arbiol, R. L. Brutchey, and M. Ibáñez, "Surface functionalization of surfactant-free particles: A strategy to tailor the properties of nanocomposites for enhanced thermoelectric performance," *Angewandte Chemie International Edition*, vol. 61, no. 35, p. e202207002, 2022.

[105] Y. Liu, S. Lee, C. Fiedler, M. C. Spadaro, C. Chang, M. Li, M. Hong, J. Arbiol, and M. Ibáñez, "Enhancing thermoelectric performance of solution-processed polycrystalline SnSe with

PbSe nanocrystals," *Chemical Engineering Journal*, vol. 490, p. 151405, 2024.

[106] M. Wu, Y. Feng, Z. Kang, Y. Wu, and X. Wang, "Transition metal-doped $SnSe_2$/$MoSe_2$ heterostructures: Modulating electronic, magnetic, and optical properties for spintronic and optoelectronic devices," *Applied Surface Science*, vol. 693, p. 162758, 2025.

[107] X. Zhang, Z. Wang, B. Zou, M. K. Brod, J. Zhu, T. Jia, G. Tang, G. J. Snyder, and Y. Zhang, "Band engineering SnTe via trivalent substitutions for enhanced thermoelectric performance," *Chemistry of Materials*, vol. 33, no. 24, pp. 9624–9637, 2021.

[108] Y. Jiang, J. Dong, H.-L. Zhuang, J. Yu, B. Su, H. Li, J. Pei, F.-H. Sun, M. Zhou, and H. Hu, "Evolution of defect structures leading to high ZT in GeTe-based thermoelectric materials," *Nature Communications*, vol. 13, no. 1, p. 6087, 2022.

[109] J. Tang, R. Zhu, Y.-H. Pai, Y. Zhao, C. Xu, and Z. Liang, "Thermoelectric modulation of neat $Ti_3C_2T_x$ MXenes by finely regulating the stacking of nanosheets," *Nano-Micro Letters*, vol. 17, no. 1, p. 93, 2025.

[110] X. Xie, "Progress in third-generation semiconductor gallium nitride (GaN): Material innovations and applications," *Guangdong Chemical Industry*, vol. 47, no. 18, p. 2, 2020.

[111] D. Shi, B. Yang, and H. Cai, "Status and trends in the development of group III nitride third generation semiconductor materials," *Science and Technology in China*, no. 04, pp. 15–18, 2018.

[112] X. Tao, W. Mu, and Z. Jia, "Advances in wide-band semiconductor gallium oxide crystals and devices," *Materials China*, vol. 39, no. 2, pp. 113–123, 2020.

[113] V. Ivady, J. Davidsson, N. Delegan, A. L. Falk, P. V. Klimov, S. J. Whiteley, S. O. Hruszkewycz, M. V. Holt, F. J. Heremans, N. T. Son et al., "Stabilization of point-defect spin qubits by quantum wells," *Nature Communications*, vol. 10, no. 1, p. 5607, 2019.

[114] Y. Wang, D. Yang, S. Wang, W. Xu, Y. Zhang, T. K. Johal, Y. Xu, Y. Wang, Y. Zhang, and Y. Zhang, "p-Type vdW Semiconductor CrSCl featuring multipolarity coexistence," *ACS Materials Letters*, vol. 7, pp. 636–645, 2025.

[115] F. Zhao, Y. He, B. Huang, T. Zhang, and H. Zhu, "A review of diamond materials and applications in power semiconductor devices," *Materials*, vol. 17, no. 14, p. 3437, 2024.

[116] X. Liu, X. Chen, D. J. Singh, R. A. Stern, J. Wu, S. Petitgirard, C. R. Bina, and S. D. Jacobsen, "Boron-oxygen complex yields n-type surface layer in semiconducting diamond," *Proceedings of the National Academy of Sciences of the United States of America*, vol. 116, no. 16, pp. 7703–7711, 2019.

[117] N. Sanders and E. Kioupakis, "Phonon- and defect-limited electron and hole mobility of diamond and cubic boron nitride: A critical comparison," *Applied Physics Letters*, vol. 119, no. 6, p. 062101, 2021.

[118] Y. Gao, D. Sun, X. Jiang, and J. Zhao, "Point defects in group III nitrides: A comparative first-principles study," *Journal of Applied Physics*, vol. 125, no. 21, p. 215705, 2019.

[119] H. Liao, C. Song, N. Yang, R. Wang, G. Tang, H. Ji, and B. Huang, "First principles study on the thermoelectric properties of GaN nanowires with C_N point defects," *Results in Physics*, vol. 52, p. 106896, 2023.

[120] E. Xu, Z. Xie, C. Cheng, X. He, W. Shen, G. Wu, K. Liang, Y. Guo, G. Ju, R. Cao et al., "Electronic structures of metal/H-diamond (111) interfaces by ab-initio studies," *Journal of Physics D: Applied Physics*, vol. 57, no. 36, p. 365102, 2024.

[121] L. Fang, X. Cao, and Z. Cao, "Chemical bonding and activity of atomically dispersed silicon in two- and three-dimensional materials," *The Journal of Physical Chemistry Letters*, vol. 14, no. 49, pp. 11125–11133, 2023.

[122] M. Liu, Y. Wang, S. Li, J. V. Anguita, S. R. P. Silva, and K. Yang, "Modulating interfacial chemistry and designing robust solid electrolyte interphases for high-performance aqueous zinc-ion batteries," *Chain*, vol. 1, no. 4, pp. 280–318, 2024.

[123] F. Lin, S.-W. Chen, J. Meng, G. Tse, X.-W. Fu, F.-J. Xu, B. Shen, Z.-M. Liao, and D.-P. Yu, "Graphene/GaN diodes for ultraviolet and visible photodetectors," *Applied Physics Letters*, vol. 105, no. 7, p. 073103, 2014.

[124] X. Yu, T. J. Marks, and A. Facchetti, "Metal oxides for optoelectronic applications," *Nature Materials*, vol. 15, no. 4, pp. 383–396, 2016.

[125] M. J. Sun, X. Cao, and Z. Cao, "$Si(C{\equiv}C)_4$-based single-crystalline semiconductor: Diamond-like superlight and superflexible wide-bandgap material for the UV photoconductive device," *ACS Applied Materials & Interfaces*, vol. 8, no. 26, pp. 16551–16554, 2016.

[126] B. Anasori, M. R. Lukatskaya, and Y. Gogotsi, "2D metal carbides and nitrides (MXenes) for energy storage," *Nature Reviews Materials*, vol. 2, no. 2, p. 16098, 2017.

[127] G. R. Bhimanapati, Z. Lin, V. Meunier, Y. Jung, J. Cha, S. Das, D. Xiao, Y. Son, M. S. Strano, V. R. Cooper et al., "Recent advances in two-dimensional materials beyond graphene," *ACS Nano*, vol. 9, no. 12, pp. 11509–11539, 2015.

[128] S. Jiang, J. Li, W. Chen, H. Yin, G. P. Zheng, and Y. Wang, "InTeI: a novel wide-bandgap 2D material with desirable stability and highly anisotropic carrier mobility," *Nanoscale*, vol. 12, no. 10, pp. 5888–5897, 2020.

[129] Y. Wu, J. Wang, G. Yuan, Y. Chen, K. Liang, D. Yang, Y. Liu, W. Luo, S. Xing, and Y. Zou, "Symmetry engineering in a 2D transition metal enables reconfigurable P-and N-type FETs,"

Nano Letters, vol. 5, pp. 1994–2001, 2025.

[130] X. Yu, P. Yu, D. Wu, B. Singh, Q. Zeng, H. Lin, W. Zhou, J. Lin, K. Suenaga, Z. Liu et al., "Atomically thin noble metal dichalcogenide: A broadband mid-infrared semiconductor," *Nature Communications*, vol. 9, no. 1, p. 1545, 2018.

[131] H. Shen, S. Liu, Y. Qiao, F. Zhang, H. Yin, and L. Ju, "High electron mobility and wide-bandgap properties in a novel 1D $PdGeS_3$ nanochain," *Physical Chemistry Chemical Physics*, vol. 24, no. 31, pp. 18868–18876, 2022.

[132] M. Ichimura, "Impurity doping in $Mg(OH)_2$ for n-type and p-type conductivity control," *Materials (Basel)*, vol. 13, no. 13, p. 2972, 2020.